博士論文 （要約）

Investigation of the role of prostanoids in acute lung injury

（急性肺障害におけるプロスタノイドの役割解明）

堀上 大貴

Contents

【Chapter 1 Introduction】

1-1 General symptoms of acute lung injury

1-1-1 Definition, cause, prevalence, and mortality rate

Acute lung injury (ALI) and its severe form acute respiratory distress syndrome (ARDS) is a respiratory disorder ($PaO_2/FiO_2 \leq 300$ mmHg) that develop within 1 week due to inflammatory stimuli such as gastric aspiration, fat embolism, bacterial mass infection, sepsis, ventilation with high tidal volume, and transfusion.[1,2] In United States, the prevalence of ALI/ARDS in patient with intensive care is 10%, and the mortality rate is high, 38.5%.[3]

1-1-2 Mechanism

In normal condition, lung exchanges gas through the alveolar wall composed of mainly type I epithelial cells, type II epithelial cells, and capillary endothelial cells. Type II epithelial cells exclude fluid from alveoli via epithelial Na^+ channels (ENaC) and cystic fibrosis transmembrane conductance regulators (CFTR). In addition, type II alveolar epithelial cells produce a lipoprotein complex, surfactant protein (SP), to inhibit the formation of lung atelectasis.

The mechanism underlying the onset and progression of ALI/ARDS has been studied for a long time since it was reported for the first time in 1967.[4] When the inflammatory stimuli initially damage bronchus, alveolar wall, and resident alveolar macrophages, the damage disrupt epithelial/endothelial barrier and impair alveolar fluid clearance. These lead lung edema formation. The inflamed endothelial cells produced angiopoietin-2 (Ang-2) which further disrupt their own barrier.[5] In addition, the macrophages stimulated upon inflammation also produce chemokines and cytokines such

as interleukin (IL)-8 (mouse homolog; C–X–C motif ligand (CXCL) 1 and CXCL2). These molecules recruit neutrophils to alveolar space and interstitial tissue, leading to neutrophil accumulation. The accumulated neutrophils disrupt lung tissue by producing reactive oxygen species (ROS). These symptoms cause the formation of shunts (unventilated blood flow regions) and lung sclerosis, resulting in respiratory dysfunction. Lung dysfunction causes death via multiple organ failure (Fig. 1).[6]

1-1-3 Treatment

In order to reduce the mortality rate of acute lung injury, several pharmacological therapies were tried. A previous clinical study showed that glucocorticoid (methylprednisolone), which was expected to reduce the excessive inflammation in lung, does not reduce the mortality rate but promotes infection via immunosuppression.[7] Other study showed that β2 adrenergic receptor agonist (salmeterol), which was expected to inhibit edema formation, aggravates ALI outcomes and increases mortality rate.[8] Another edema inhibitor, phosphodiesterase (PDE) 5 inhibitor (sildenafil), decreases the pressure of pulmonary artery of ALI patients, but not reduces the mortality rate.[9] Zeiher *et al.* showed that neutrophil elastase inhibition (sivelestat) does not improved the survival rate.[10] These is no effective pharmacological therapy against ALI/ARDS. Thus, there are only supportive therapies such as protective ventilation with low tidal volume and prone positioning.[11,12]

1-2 Experimental ALI models

Again, ALI/ARDS is caused by various stimuli such as gastric aspiration, fat embolism, bacterial mass infection, sepsis, ventilation with high tidal volume, and

transfusion. Thus, investigators have been using several types of experimental ALI models to mimic the human ALI/ARDS. These experimental ALI models have different mechanisms in pathological progression. I explain each model as below.

Hydrochloric acid-induced ALI model: Hydrochloric acid (HCl)-induced ALI model using rat, or mice is made by the intra-nasal or intratracheal administration of HCl, which mimics human ALI/ARDS caused by aspiration of gastric contents.[13,14] Administrated HCl initially damages bronchial and alveolar epithelium, causing necrosis. Zarbock *et al.* showed that the administration of HCl to mice exhibits both edema formation and neutrophil accumulation accompanied with respiratory dysfunction.[14]

Oleic acid-induced ALI model: Oleic acid (OA)-induced ALI model using dog, guinea-pig, and mice is made by the intravenous administration of emulsified OA.[15-17] This model mimics human ALI/ARDS caused by fat embolism. Schuster *et al.* showed that the intravenous administration of OA to dog induces necrosis of endothelial cells by mediating vacuolation, resulting in severe edema formation.[15]

Lipopolysaccharide-induced ALI model: Lipopolysaccharide (LPS)-induced ALI model using sheep, rat, and mice is made by the intra-nasal or intratracheal administration of LPS.[18-20] This model mimics human ALI/ARDS caused by bacterial mass infection. Kabir *et al.* showed that the intratracheal injection of LPS to mice increases the level of inflammatory cytokines, leading severe neutrophil accumulation in lung.[20]

LPS+OA-induced ALI model: Double-hitting ALI models by administrating of LPS and

OA using mouse is utilized to mimic human ALI/ARDS caused by fat-embolism and mass infection together.[21] Voelker *et al.* showed that this LPS+OA-induced ALI mice model exhibits severe edema formation and neutrophil accumulation compared with the single administration of LPS or OA.[21]

Sepsis-induced ALI model: Sepsis-induced ALI model using dog and mice is made by the intravenous or intraperitoneal administration of LPS.[22,23] This model mimics sepsis shock-induce human ALI/ARDS. Kawasaki *et al.* showed that administrated LPS increased the plasma cytokines, leading pulmonary inflammation.[23]

Ventilation-related ALI model: Ventilation-related ALI model using mice is made by the ventilation with high tidal volume, which is observed in the clinical condition.[24] Birukova *et al.* showed that injected air mechanically widen the alveolar wall, leading both edema formation and neutrophil accumulation.[24]

Transfusion-related ALI model: Transfusion-related ALI model using mice is made by the intravenous administration of the passive transfusion of an MHC class I (MHC I) mAb ($H2K^d$) to mice with the cognate antigen.[25] This model mimics human ALI/ARDS developed after the transfusion of a plasma-containing blood product. Looney *et al.* showed that the administration of MHC I mAb causes both edema formation and neutrophil accumulation.[25]

Other ALI models: There are other experimental ALI models. Cuzzocrea *et al.* showed that the administration of carrageenan (a high-molecular-weight sulphated

polysaccharide) into pleural cavity of rat caused pleurisy and lung injury accompanied with edema formation and neutrophil accumulation.[26] Goggel *et al.* showed that the intratracheal administration of platelet activating factor (PAF) to isolated rat lung caused edema formation.[27]

1-3 The effect of vascular permeability

A blood vessel maintains the homeostasis of the tissues by preventing the passage of macromolecules exceeding 40 kDa. However, when inflammatory stimuli increase vascular permeability, protein-rich fluid including fibrinogen, globulin, and albumin extravasate to the inflamed tissue, leading to edema formation. Vascular permeability is controlled by the functions of two types of cells, endothelial cells and vascular mural cells.

1-3-1 Endothelial cells in vascular permeability

Endothelial cells cover luminal side of a blood vessel with a single layer. In the normal conditions, endothelial cells form “adherence junction” composed of VE-cadherin and “cortical actin rim” composed of f-actin. These structures enhance endothelial barrier, which decreases vascular permeability. In the inflammatory condition, VE-cadherin is internalized into cells and f-actin forms “stress fiber” which contract cell inward. These changes disrupt endothelial barrier, increasing vascular permeability.

1-3-2 Vascular mural cells in vascular permeability

Vascular mural cells cover the outside of endothelial cells in the single or several layer. The number of the layer differs depending on the type of vessels. In proximal

vessels, vascular smooth muscle cells consist vascular wall in several layer. In the distal vessels, pericytes form vascular wall in single-layer. Capillaries has no vascular mural cells.

Vascular smooth muscle cells have actomyosin filament composed of myosin light chain (MLC) and actin filament. When vasoconstrictor stimulates vascular smooth muscle cells, MLC kinase (MLCK) phosphorylate MLC, leading vasocontraction by the attraction between MLC and actin filament. Vasocontraction reduces the blood flow into downstream tissues and hydrostatic pressure on the vessel wall, decreasing vascular permeability. On the other hand, when vasodilator stimulates vascular smooth muscle cell, myosin light chain phosphatase (MLCP) dephosphorylate MLC. The dephosphorylation release the binding between MLC and actin filament, resulting in vasorelaxation. The relaxation of blood vessels increases the blood flow and hydrostatic pressure, increasing vascular permeability.

1-4 Neutrophil accumulation

Neutrophils are one type of white blood cells which play an important role in innate immunity. Neutrophils also play an important role in acute inflammation. Inflammatory stimuli cause neutrophil accumulation through two types of pathway; neutrophil transmigration and adhesion molecules in endothelial cells.

Neutrophils are spherical in the normal condition. The stimulation on neutrophils causes the formation of the lamellipodia via a f-actin polymerization on the stimulated side and the contraction of actomyosin filament via MLCK on the opposite side. By these phenomena, neutrophils transmigrate through vessel wall.

Endothelial cells express adhesion molecules such as p-selectin, intercellular

adhesion molecule (ICAM)-1 and vascular cell adhesion molecule (VCAM)-1. The stimulation on endothelial cells increases the level of these adhesion molecules. P-selectin capture platelet/endothelial cell adhesion molecule (PSGL) 1 expressed on circulating neutrophil (rolling), leading to rolling of neutrophils. ICAM-1 and VCAM-1 induce adhesion and crawling of rolling neutrophils. These steps (rolling, adhesion, and crawling) promotes neutrophil transmigration.

1-5 Prostanoids

Prostanoids are lipid mediators which govern inflammatory reactions in our body. They are synthesized from cell membrane-derived arachidonic acid via two types of cyclooxygenases (COX1 and COX2) and specific prostaglandin (PG) or thromboxane (TX) synthases (Fig. 2). There are five major prostanoids; PGE_2, PGI_2, TXA_2, $PGF_{2\alpha}$, and PGD_2. These prostanoids bind to their specific receptors.

Since abundant prostanoids were detected in lung tissue or plasma of ALI patients,[28,29], researchers have investigated the therapeutic effect of COX inhibition on ALI.

1-5-1 The effect of COX inhibition on ALI progression

Several studies showed that COX inhibition has a therapeutic effect against ALI progression in experimental studies. Hinshaw *et al.* firstly showed the treatment with COX1 and COX2 inhibitor (aspirin) attenuates the mortality rate in sepsis-induced dog ALI model.[22] In both transfusion-related ALI mice model and LPS-induced ALI mice model, the treatment with aspirin attenuates edema formation and neutrophil accumulation.[30,31] In carrageenan-induced ALI rat model, COX2 inhibition by

celecoxib attenuates edema formation and neutrophil accumulation.[26]

On the other hand, there are other studies which showed that inhibition or gene deficiency of COX do not attenuate ALI progression. Fukunaga *et al.* showed that the treatment with COX2 inhibitor (NS-398) and gene deficiency of COX2 aggravates edema formation and neutrophil accumulation in HCl-induced mice model.[13] In clinical trial, the group of Bernard showed that the treatment with COX2 inhibitor (ibuprofen) does not reduce the mortality rate of ALI patients.[32] In addition, clinical study also showed that the treatment with aspirin does not affect the mortality rate of ALI patients.[33]

These findings indicate that COX inhibition has both pro- and anti-inflammatory effect on ALI progression. The effect of COX inhibition might be affected by the type of stimuli and animal species. In order to reveal the complexity, detail investigation focusing on the role of each COX-metabolite prostanoid in the progression of ALI is needed.

1-5-2 Multiple role of prostanoids in ALI progression

There are several studies showing pro-inflammatory role of prostanoids in ALI progression. Goggel *et al.* showed that gene deficiency of a PGE_2 receptor EP3, reduced the platelet activation factor-induced pulmonary edema formation.[27] The treatment with the specific TXA_2 receptor (T-prostanoid (TP) receptor) antagonist (SQ29548) attenuates the HCl-induced lung edema formation, neutrophil accumulation, and respiratory dysfunction.[14] The treatment with thromboxane synthase (TXS) inhibitor (ozagrel) also attenuates lung edema formation and neutrophil accumulation in OA-induced ALI of guinea-pig.[16]

On the other hand, there are several studies showing anti-inflammatory reactions of prostanoids in ALI. In the ventilation-related ALI mice model, the treatment with PGE_2

or PGI_2 analog (beraprost) attenuates the lung edema formation and neutrophil accumulation.[24] The treatment with an agonist for PGE_2 receptor EP4 attenuated the lung edema formation and neutrophil accumulation in LPS-induced ALI of mice.[34] Gene deficiency of EP4 receptor, but not EP1-3 receptor, aggravated the LPS-induced airway inflammation in mice.[35] Our group previously showed that gene deficiency of hematopoietic prostaglandin D synthase H-PGDS accelerated the lung edema formation and neutrophil accumulation.[36] Our group also reported that H-PGDS-derived PGD_2 attenuates ALI via D-prostanoid (DP) receptor in both LPS- and LPA+OA-induced ALI mice models.[36]

These studies indicate that there are both pro- and anti-inflammatory prostanoids in ALI progression. However, there are still unclear points; the contribution of each prostanoid to ALI promotion or attenuation, the differences in the role of prostanoids due to differences in models, and the type of cells expressing its enzymes and receptors. By revealing these points, I would establish the new therapeutic strategy instead of COX inhibition.

1-6 Objective

In this study, I conducted a study to clarify the role of prostanoids (TXS-derived TXA_2 and L-PGDS-derived PGD_2) in ALI progression. I investigated how much these prostanoids are produced and how they work in ALI progression depending on the stimulus, model, and stage.

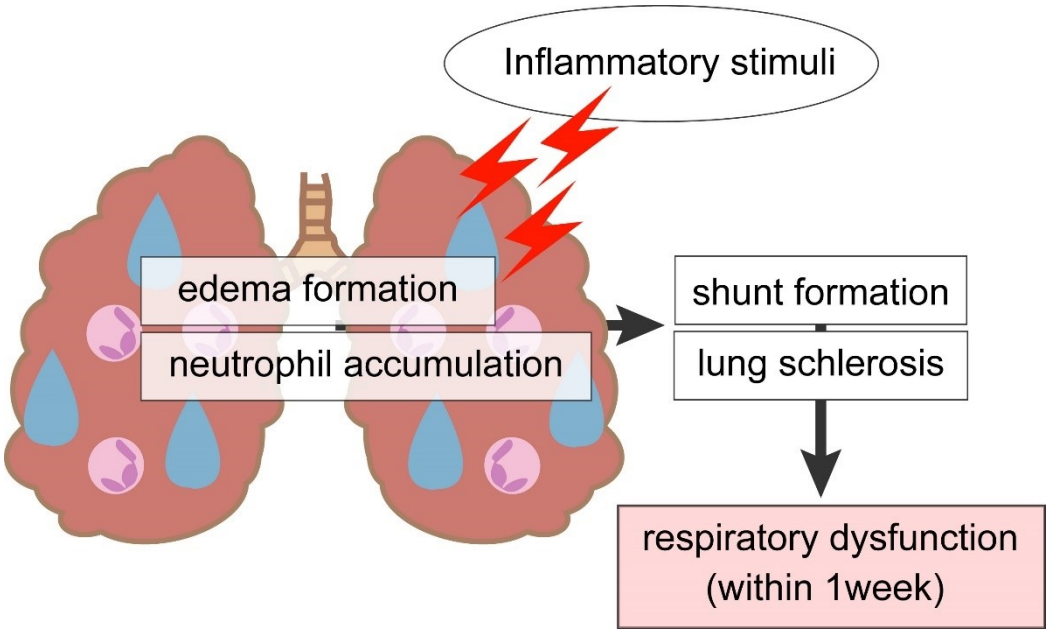

Figure 1. The mechanism in ALI progression

Exogenous inflammatory stimuli such as aspiration of gastric contents firstly damages bronchi and alveoli. The damage causes characteristic ALI symptoms; edema formation and neutrophil accumulation, resulting in shunt formation and increase of lung elastance. These symptoms finally induce respiratory dysfunction within 1 week.

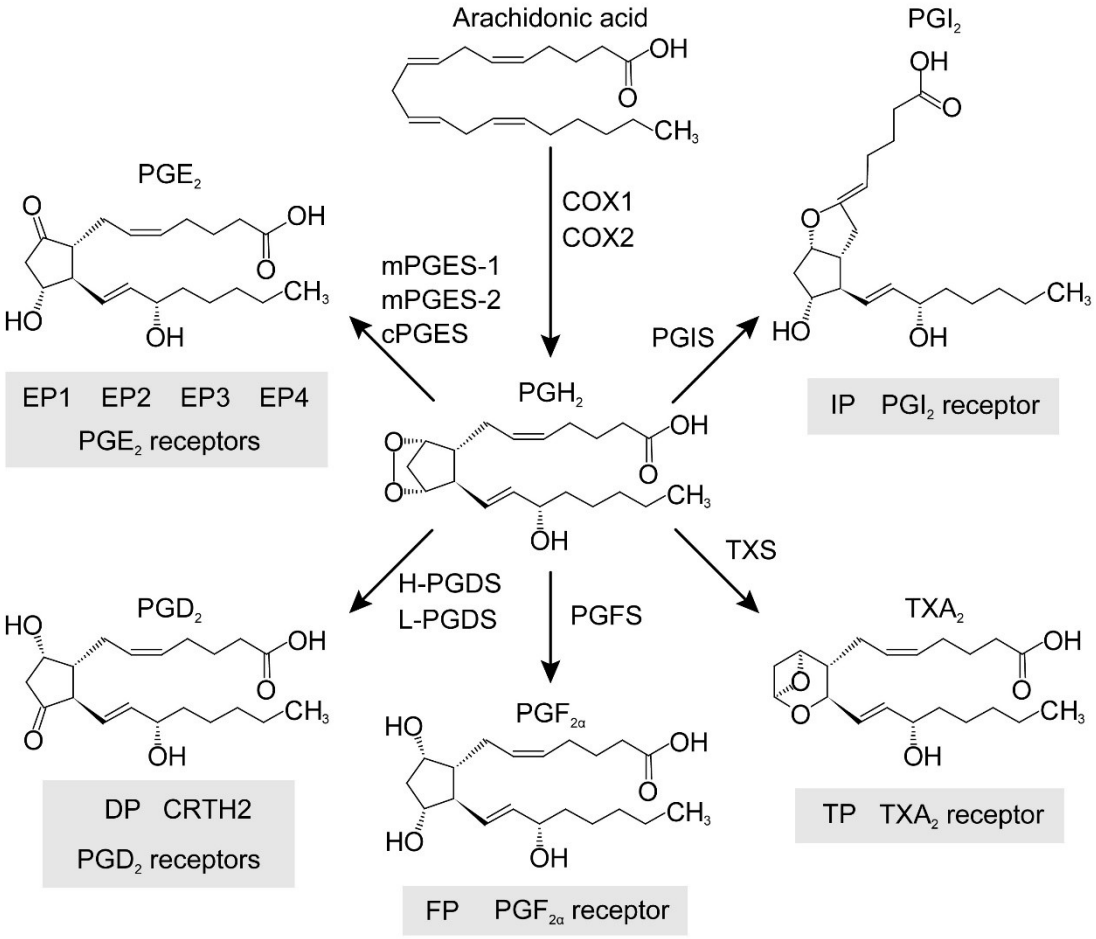

Figure 2. Synthetic pathways and receptors of prostanoids

PGH_2 is produced from arachidonic acid by the activity of COX1 or 2. Then produced PGH_2 is metabolized to PGE_2, PGI_2, PGD_2, $PGF_{2\alpha}$, and TXA_2 by specific prostanoid synthases. These prostanoids have 20 carbon including 5- or 6-membered ring, 2 side chains, and 2 double bonds and bind to their specific G-protein coupled receptors (GPCRs).

【Chapter 2 The role of TXA_2 in ALI】

2-1 Introduction and objective

2-1-1 TXA_2

TXA_2 is one of major prostanoids produced by TXS and binds to its specific GPCR, TP receptor coupling to G_q or G_{12} (Fig. 2). TXA_2 is known to cause vasocontraction and platelet aggregation.

2-1-2 TXA_2 and disease

In vivo studies indicated that TXA_2 has pro-inflammatory role in disease progression. In the catheter-induced carotid vascular injury mice model, gene deficiency of TP receptor depressed the injury-induced vascular proliferation.[37] The treatment with TP antagonist (S188856) attenuates renal oxidant stress and proteinuria in diabetic apolipoprotein E-deficient mice.[38]

2-1-3 TXA_2 and ALI

As described above, some studies show the pro-inflammatory role of TXA_2 in ALI progression as well as other disease. In the HCl-induced ALI mice model, the treatment with TP receptor antagonist (SQ29548) reduces respiratory dysfunction.[14] Ishitsuka *et al.* showed that the treatment with TXS inhibitor (ozagrel) attenuates respiratory dysfunction in OA-induced ALI guinea-pig model.[16] In the clinical trials, Yu *et al.* showed that the pretreatment with TXS inhibitor (ketoconazole) to septic patients prevent the development of ALI and the mortality rate.[39] . These studies suggest that TXS-TXA_2-TP receptor pathway aggravates ALI progression. However, the type of cells expressing TXS and TP receptor and detailed mechanism how TXA_2 aggravates ALI are

unknown.

2-1-4 TXA_2 and vascular permeability

TXA_2 is known to cause vasocontraction and endothelial barrier disruption. The treatment with TP agonist (U46619) strongly causes the vasocontraction of human umbilical vein, rat middle cerebral artery, human retinal capillary, and human uterine artery.[40-43] In addition, TP stimulation disrupts endothelial barrier of bovine aortic endothelial cells and HUVECs.[44,45]

These results show that TXA_2 can decreases vascular permeability via vasocontraction and increases vascular permeability via endothelial barrier disruption. However, the effect of TXA_2 on vascular permeability *in vivo* is unknown.

2-1-5 Objective

In this chapter, I conducted a study to clarify the role of TXA_2-TP signaling in ALI progression. I investigated how much TXA_2 produced and how they work in ALI progression depending on the type of stimuli.

2-2 Material and Methods

2-2-1 Animals

All the experiments were approved by the Institutional Animal Care and Use Committee of the University of Tokyo. All experimental methods were performed with the approved guidelines. C57BL6J mice and Balb/c mice were purchased from CLEA Japan Inc. (Tokyo, Japan). Male (6-12 weeks old) C57BL6J mice were used for the experiments using mice lung, while male (8 weeks old) Balb/c mice were used for the experiments using mice ear.

2-2-2 Experiments using mice lung

Experimental model of ALI

C57BL6J mice were anesthetized and maintained with 2% isoflurane on a heating pad. To make the acid aspiration- or severe infection-induced ALI model, HCl (0.1 M; 2.5 μl/g, intra-nasally) or LPS (3.75 mg/kg, 2.5 μl/g, intra-nasally) was administrated. To make the fat embolism-induced ALI model, LPS (1.5 mg/kg, intra-nasally) and OA (0.15 ml/kg dissolved in 0.1% bovine serum albumin solution, intravenously, 30 min after LPS administration) were administrated. Six hours after the administration with HCl or LPS, mice were euthanized and lungs were immediately perfused with physiological salt solution (136.9 mM NaCl, 5.4 mM KCl, 5.5 mM, 23.8 mM $NaHCO_3$, 1.5 mM $CaCl_2$, 1.0 mM $MgCl_2$, and 0.01 mM EDTA) and used for further experiments. Vehicle-treated group received saline instead of HCl, LPS, or OA treatment.

Measurement of SpO_2

Before euthanasia, mice were anesthetized on a heating pad and then the

MouseOx collar clip was put on the shaved neck. A pulse oximeter system (STARR Life Sciences, Allison Park, PA, USA) was used to monitor SpO_2. After 3-5 min, the readings of pulse oximetry were recorded (1 min, 1 reading/s). The mean value of the recorded readings was used for data analysis.

CT analysis

Before euthanasia, mice were anesthetized and scanned with the micro-CT system (LaTheta LCT-200, Aloka, Tokyo, Japan). The voxel size was 48 × 48 μm, the interval was 192 μm, and X-ray voltage was 50 kV. The scanned data was analyzed and reconstructed as the cross section of lung in the Latheta software.

Measurement of prostanoids

To measure TXB_2, 6-keto-$PGF_{1\alpha}$, and PGE_2 in bronchi alveolar lavage fluid (BALF), mice were euthanized and BALF was collected with 1 ml saline. After the centrifugation (4℃, 5 min, 5000×g), supernatant was collected.

The supernatants were mixed with distilled water, ethanol, HCl, and internal standards. As internal standards, TXB_2-d4, 6-keto-$PGF_{1\alpha}$-d4, PGE_2-d4, (Cayman chemical, Ann Arbor, MI, USA) were used. Mixed samples were purified with solid phase extraction cartridge (Sep-Pak C18 3 cc Vac Cartridge, Waters, Milford, MA, USA) and eluted. The eluate was dried and dissolved with 10% acetonitrile in distilled water.

Prostanoids in the dissolved solutions were measured using the liquid chromatography-mass spectrometry system (LCMS-8030, Shimadzu, Kyoto, Japan). The Inertsil ODS-3 column (GL Sciences, Tokyo, Japan) and the mobile phase composed of acetonitrile and 0.02% acetic acid in distilled water were used for the liquid

chromatographic separation. The concentration of each prostanoid were calculated by the dividing the level of detected prostanoid by the amount of BALF.

Measurement of water content

Excised lungs were weighted to get the wet weight. After drying in the oven (55℃, 48 h), the samples were reweighted to get the dry weight. The water content was calculated by dividing the wet weight by the dry weight or the amount of evaporated water by the mouse body weight.

Measurement of MPO activity

Excised lungs were homogenized in 0.3% hexadecyl trimethyl ammonium bromide in potassium phosphate buffer (pH 6.0, 5 mM K_2HPO_4, 45 mM KH_2PO_4). After centrifugation (4℃, 30 min, 20000×g), supernatant was collected. Collected samples were incubated with 0.5 mM *o*-dianisidine dihydrochloride (MP Biochemicals, Solon, OH, USA) and 0.05% hydrogen peroxide. After 5 min incubation, the level of MPO was measured as the absorbance at 450 nm using the plate reader (ARVO-SX 1420, PerkinElmer, Waltham, MA, USA). MPO activity was calculated by dividing the level of MPO by the protein concentration.

2-2-3 Experiments using mice ear

Miles assay

Balb/c mice were anesthetized and put on a heating pad. To perform Miles assay in ear, Evans blue dye (50 mg/kg) was injected immediately after the U46619 (20 or 200 μg in methyl acetate) administration. After 30 min circulation, ears were excised.

The excised lungs or ears were dried and weighted. The extravasated dye were extracted from dried samples by incubating with formamide (55℃, o/n). The extracted dye was measured as the absorbance at 650 nm using the plate reader.

Intravital imaging

Balb/c mice were anesthetized and put on a heating pad. Fluorescein isothiocyanate–dextran (FITC-dextran, 66,100 Da, 40 mg/kg) was injected intra-venously and then U46619 (20 μg) was applied onto the auricle. The diameter of artery or vein and the leakage of FITC-dextran were observed every 5 min with confocal microscope (ECLIPSE Ti with C1 confocal system, Nikon, Tokyo, Japan) and quantified with EZ-C1 software (Nikon, Tokyo, Japan).

Measurement of blood flow

Balb/c mice were anesthetized and put on a heating pad. After 20 min application with U46619 (20 μg) onto the auricle, the blood flow of murine ear was visualized using the a 2D laser speckle flowmetry (OZ-1, Omegawave Inc., Tokyo, Japan). The change of blood flow was calculated as the difference of the intensity between the stimulated ear and the control ear.

2-2-4 *In vitro* assay

Cell culture

HUVECs, HPAECs, and HMVECs were purchased from Lonza (Basel, Switzerland, passage 4-8) These cells were cultured in Endothelial Cell Growth Medium-2 (EGM-2). After 4 h starvation with Endothelial Cell Basal Medium-2 (EBM-2) with

2% fetal bovine serum (FBS), The cells were used for the experiments.

The measurement of trans-endothelial resistance (TEndR)

TEndR were measured using the xCELLigence Real-Time Cell Analyzer System (Roche, Basel, Switzerland). Cells (1×10^4) were seeded onto electrodes and incubated for 24 h. After the starvation, each agonist was administrated and then TEndR was monitored every 5 min. The value of TEndR was expressed as the ratio to the initial value 30 min or 5 min before the administration.

Transwell permeability assay

HUVECs (8×10^4) were seeded onto the top chamber of the transwell (1 μm pore size, BD Biosciences, Bedford, MA, USA) and cultured until confluent. After the starvation, U46619 (0.1-1 μM) and FITC dextran (70,000 Da, 24 μg) were administrated into the top chamber (300 μl). The FITC dextran infiltrated to the bottom chamber (900 μl) was collected every 10 min after the administration. The infiltrated FITC dextran was measured as the excitation/emission wavelengths of 485/535 nm using the plate reader.

2-2-5 Pathological analysis

Morphological analysis

Lungs were excised and fixed with 4% paraformaldehyde (PFA) or Bouin's solution for 24 h. Paraffin section (4 μm) of fixed lungs were used for hematoxylin and eosin (H&E) staining or Alcian blue staining. Stained sections were observed in the light microscope (Optihot-2, Nikon, Tokyo, Japan).

Immunohistochemistry using lung tissue

Lungs were excised and fixed with 4% PFA or Bouin's solution for 24 h. Fixed lungs were embedded into OCT compound (Sakura FineTek Japan, Tokyo, Japan) and then frozen sections (4 or 5 μm) were made. The sections were permeabilized and blocked with 0.1 or 0.3% Triton X-100 and 3% normal goat serum for 30 min followed by the incubation (4℃, o/n) with primary antibodies: rat anti-CD41 (1:200, MWReg30, MCA2245; AbD Serotec, Kidlington, UK), rat anti-E-cadherin antibody (1:200, DECMA-1147302; Biolegend, San Diego, CA, USA), and rabbit anti-TXS antibody (1:100, OTI2C1, ab39362; Abcam, Cambridge, UK). Then, sections were incubated (3 h) with the secondary antibodies (1:500): Alexa Fluor® 488 goat anti-rat antibody (A11006) and Alexa Fluor® 568 goat anti-rabbit antibody (A11011; Invitrogen, Carlsbad, CA, USA). Nuclei were stained with DAPI (4',6-diamidino-2-phenylindole) and then the sections were observed in the fluorescence microscope (Eclipse E800, Nikon, Tokyo, Japan).

For DAB (3,3'-diaminobenzimide tetrahydrochloride) staining, frozen sections were incubated with rabbit anti-TXS antibody (1:100) and then labeled with biotinylated goat anti-rabbit IgG (1:500, BA1000; Vector Laboratories Inc., Burlingame, CA, USA), VECTASTAIN ABC Kit (Vector Laboratries Inc.), and 0.02% DAB (Dojindo, Kumamoto, Japan). Nuclei were stained with hematoxylin and stained sections were observed in the light microscope.

Immunohistochemistry using ear, pulmonary artery, and cells

For ear staining, mice stimulated with U46619 and histamine were euthanized and ears were perfused and fixed with 4% PFA for 15 min. For staining of pulmonary

artery, mice were euthanized and excised pulmonary artery was stimulated with U46619 and histamine and then fixed with 4% PFA for 15 min. For cell staining, HUVECs were seeded onto the cover glass coated by gelatin. Starved cells were stimulated with U46619 and fixed with 4% PFA for 5 min. Fixed ear, pulmonary artery, and cells were permeabilized and blocked with 0.1 or 0.3% Triton X-100 and 3% bovine serum albumin for 30 min followed by the incubation (4℃, o/n) with primary antibodies: goat anti-VE-cadherin antibody (1:200; Santa Cruz, Dallas, Texas, USA). The sections were labeled with rhodamine-phalloidin (3:100; Life Technologies, Carlsbad, CA, USA) and donkey anti-goat IgG (1;200) for 1 h. Nuclei were stained with DAPI and then the sections were observed in the fluorescence microscope.

2-2-6 Statistic analysis

The all results were shown as mean ± S.E.M. Statistical difference of the groups were determined using t-test for two-group comparisons and one-way ANOVA followed by Turkey's test for multiple-group comparisons. $P<0.05$ was considered as significant.

2-3 The role of TXA_2-TP signaling in HCl-induced ALI

Firstly, I investigated the role of TXA_2-TP signaling in HCl-induced ALI. The administration of HCl (0.1 M, 2.5 μl/g, intra-nasally, 6 h) induced hemorrhage (White dotted line, Fig. 3A). Computed tomography (CT) scan demonstrated that HCl administration caused infiltrative shadow around bronchi indicating lung inflammation (Fig. 3B, arrowhead). The treatment with TP receptor antagonist (SQ29548, 2 mg/kg, intraperitoneally, 0, 2, and 4 h after HCl administration) significantly attenuated these symptoms. HCl administration also caused respiratory dysfunction shown as the decrease of peripheral oxygen saturation (SpO_2, Fig. 3C; vehicle, -2.50 ± 0.74%; HCl, -17.30 ± 2.72%). The treatment with SQ29548 significantly attenuated the lung dysfunction (-8.64 ± 2.09%).

I next evaluated the level of TXA_2 by measuring a stable metabolite of TXA_2, TXB_2. TXB_2 was not detected in BALF of vehicle-administrated mice. HCl administration induced TXB_2 production in BALF (Fig. 3D; HCl, 284 ± 118 pg/ml). The administration of HCl also increased the level of BALF PGE_2 (Fig. 3E; vehicle, 3.8 ± 3.8 pg/ml; HCl, 1619 ± 496 pg/ml), but not that of BALF 6-keto $PGF_{1\alpha}$ (a metabolite of PGI_2, Fig. 3F; vehicle, 77.4 ± 0.1 pg/ml; HCl, 79.8 ± 2.0 pg/ml).

These results suggested that the administration of HCl induces TXA_2 production which aggravates ALI via TP receptor.

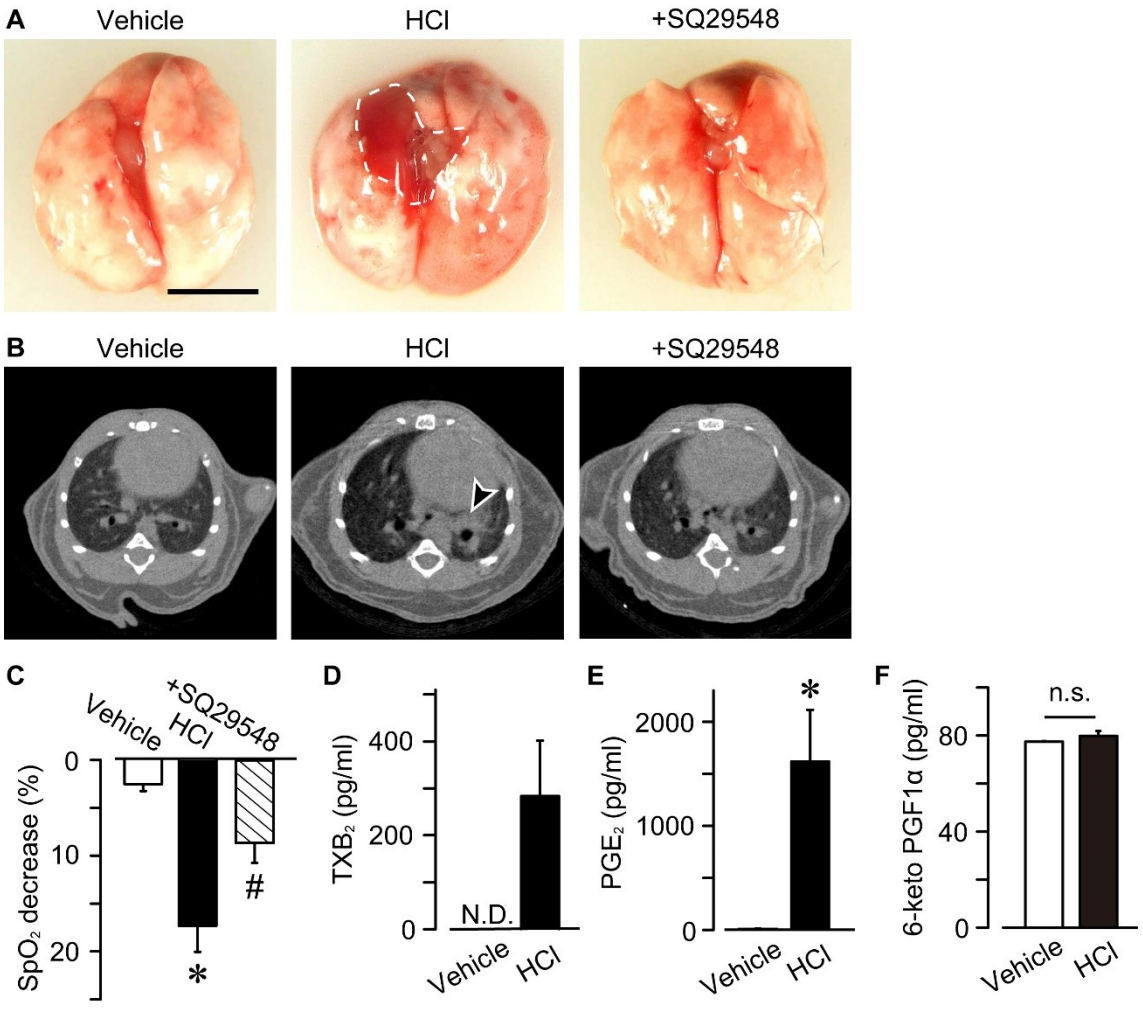

Figure 3. TXA_2-TP signaling aggravated HCl-induced ALI

SQ29548 (2 mg/kg, intraperitoneally, 0, 2, and 4 h after HCl administration) was treated to HCl-administrated mice (0.1 M, 2.5 μl/g, intra-nasally, 6 h). (A) Representative pictures of perfused and excised lungs (n=8-14). White dotted line indicates the area of hemorrhage. Bar = 5.0 mm. (B) Representative pictures of the cross section of inflamed lung scanned by computed tomography (CT, n=5-8). Arrowheads indicate infiltrative shadow. (C) Summary of SpO_2 (n=6-12). (D-F) The concentration of (D) TXB_2 (n=5 each), (E) PGE_2 (n=5 each), and (F) 6-keto $PGF_{1\alpha}$ (n=5-6) in BALF. Data are represented as mean ± SEM. *p<0.05 compared with vehicle-administrated mice. n.s., not significant.

2-4 The role of TXA_2-TP signaling in HCl-induced edema formation and neutrophil accumulation

I investigated the pathophysiological mechanism of TXA_2-TP receptor signaling-induced ALI aggravation. In the morphological study, HCl-administrated lung exhibited inflammation especially around the bronchi accompanied with disruption of alveolar wall, protein extravasation (black arrowheads) and neutrophil accumulation (white arrowheads, middle panels, Fig. 4A). The treatment with SQ29548 attenuated the inflammation and edema formation, but not neutrophil accumulation (right panels). This result suggested that TXA_2-TP receptor signaling cause edema formation rather than neutrophil accumulation.

Next, I evaluated the level of characteristic symptoms: edema formation and neutrophil accumulation. HCl administration increased both water content, the indication of edema formation, and myeloperoxidase (MPO) activity, the indication of neutrophil accumulation (Fig. 4B and C). The treatment with SQ29548 significantly decreased water content, but not MPO activity. In addition, the administration of TP receptor agonist (U46619, 25 μg/kg, intra-nasally,1 h) significantly increased water content, but not MPO activity (Fig. 4D and E).

These results indicated that TXA_2-TP signaling aggravates HCl-induced ALI via edema formation.

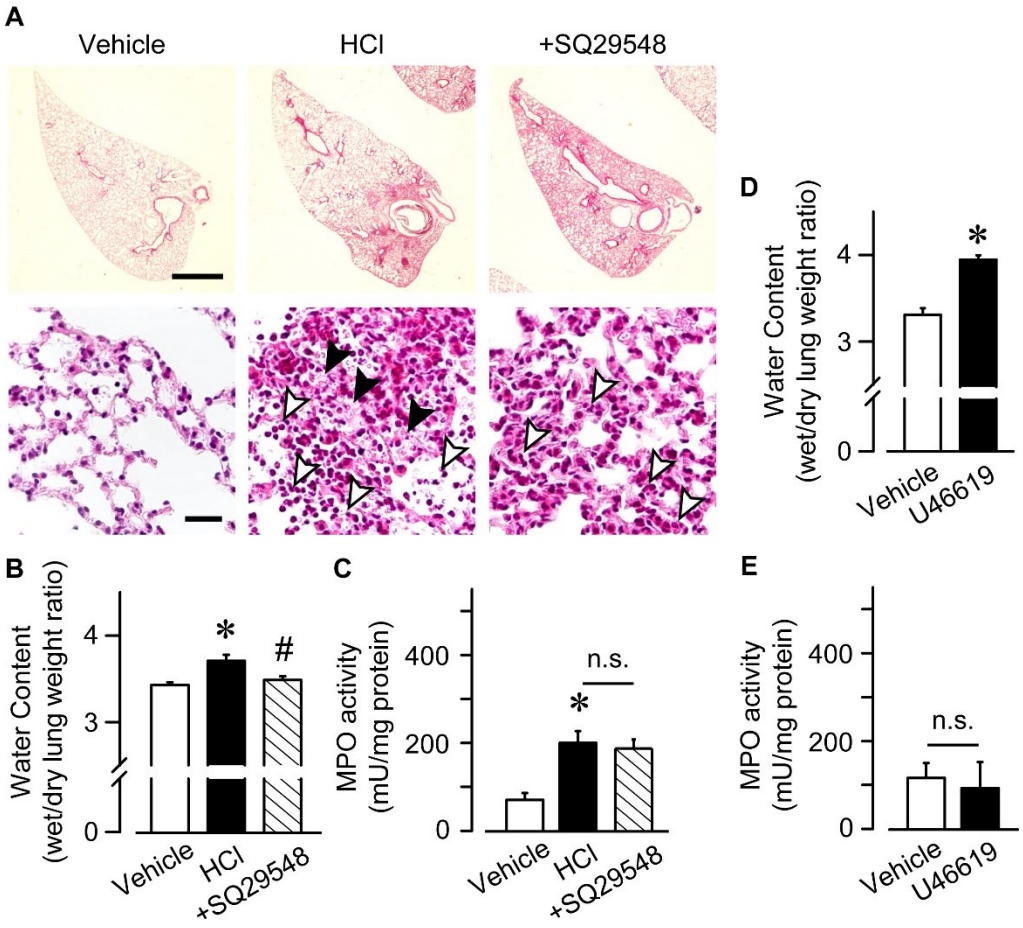

Figure 4. TXA$_2$-TP signaling promoted edema formation in HCl-induced ALI

(A-C) SQ29548 (2 mg/kg, intraperitoneally, 0, 2, and 4 h after HCl administration) was treated to HCl-administrated mice (0.1 M, 2.5 μl/g, intra-nasally, 6 h). (A) Representative pictures of hematoxylin and eosin (H&E) stained lung section (n=7 each). Bar = 1.0 mm or 20 μm. Black arrowheads indicate protein extravasation and white arrowheads indicate neutrophil accumulation. (B) Summary of water content (n=5-7). (C) Summary of MPO activity (n=8 each). (D-E) U46619 (25 μg/kg, intra-nasally, 1 h) was administrated to mice. (D) Summary of water content (n=6-7). (E) Summary of MPO activity (n=4-5). Data are represented as mean ± SEM. *$p<0.05$ compared with vehicle-administrated group. #$p<0.05$ compared with HCl-administrated group. n.s., not significant.

2-5 TXS expression in HCl-administrated lung tissue

I investigated the type of cells which express TXS in HCl-induced ALI model. Immunohistochemical study by DAB (3,3'-diaminobenzidine) staining showed that, in the HCl-administrated lung, TXS was expressed on both bronchus and alveolar wall (Fig. 5A, right panel). Non-specific staining of DAB was not observed in negative controls which was incubated without primary antibody (left panel).

Furthermore, immunofluorescent study showed that TXS was not expressed in the vehicle-administrated lung, while TXS was expressed on E-cadherin positive epithelial cells in the HCl-administrated lung (Fig. 5B). On the other hand, TXS expression was observed in CD41-positive platelets (Fig. 5C).

These results suggested that bronchi and alveolar epithelial cells express TXS.

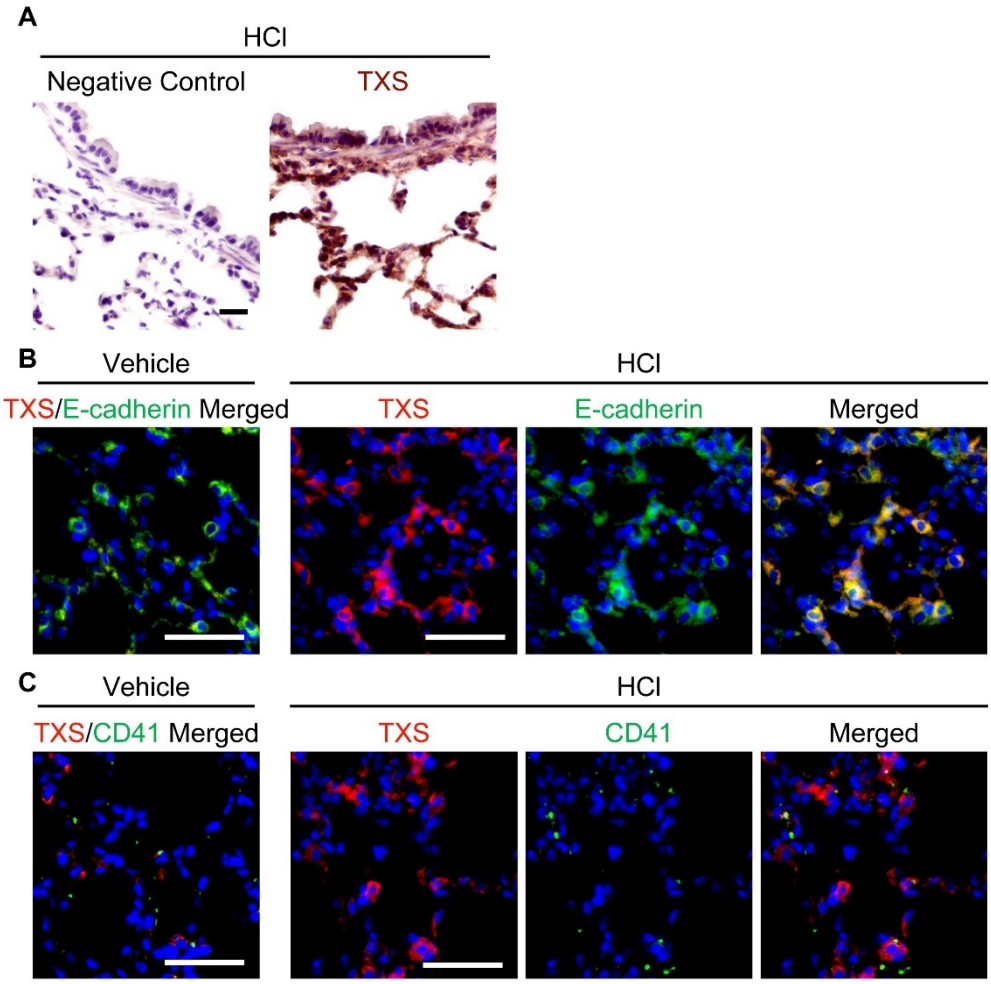

Figure 5. Inflamed lung epithelial cells expressed TXS

After the administrated of HCl (0.1 M, 2.5 μl/g, intra-nasally) for 6 h, lungs were excised, fixed, and then used for immunostaining. (A) Representative pictures of DAB staining of TXS in HCl-administrated lung section (right panel, n=4). Left panel shows the negative control which was incubated without primary antibody (left panel, n=4). Bar = 20 μm. (B-C) Representative pictures of immunofluorescence staining of TXS (red) and (B) E-cadherin (green) or (C) CD41 (green) in vehicle- or HCl-administrated lung section (n=4 each). Panels in vehicle groups and right panels in HCl groups show the merged pictures. Bar = 50 μm.

2-6 The role of TXS-TXA_2-TP signaling in LPS+OA-induced ALI

2-6-1 The role of TXS-TXA_2-TP signaling in LPS+OA-induced ALI

I investigated the role of TXA_2-TP signaling on another experimental ALI model, LPS+OA-induced ALI model. The administration of LPS (1.5 mg/kg, intranasally, 6 h) and OA (150 μl/g, intravenously, 30 min after LPS administration) caused severe extensive hemorrhage and infiltrated shadow in lung tissue compared with HCl-induced ALI model (Fig. 6A and B). However, LPS+OA administration did not cause lung dysfunction (Fig. 6C). Both the treatment with not only SQ29548 (2 mg/kg, intraperitoneally, 0, 2, and 4 h after HCl administration) but also TXS inhibitor (ozagrel, 50 mg/kg, intraperitoneally, 15 min after LPS administration) attenuated the lung hemorrhage and the formation of infiltrative shadow.

As well as HCl administration, LPS+OA administration increased the level of BALF TXB_2 (Fig. 6D; vehicle, 72.2±72.2 pg/ml; LPS+OA, 359±94 pg/ml), which was decreased by the treatment with ozagrel, but not by the treatment with SQ29548. The level of BALF PGE_2 was not increased significantly by the LPS+OA administration (Fig. 6E).

These results suggest that TXS-TXA_2-TP signaling aggravates LPS+OA-induced lung inflammation.

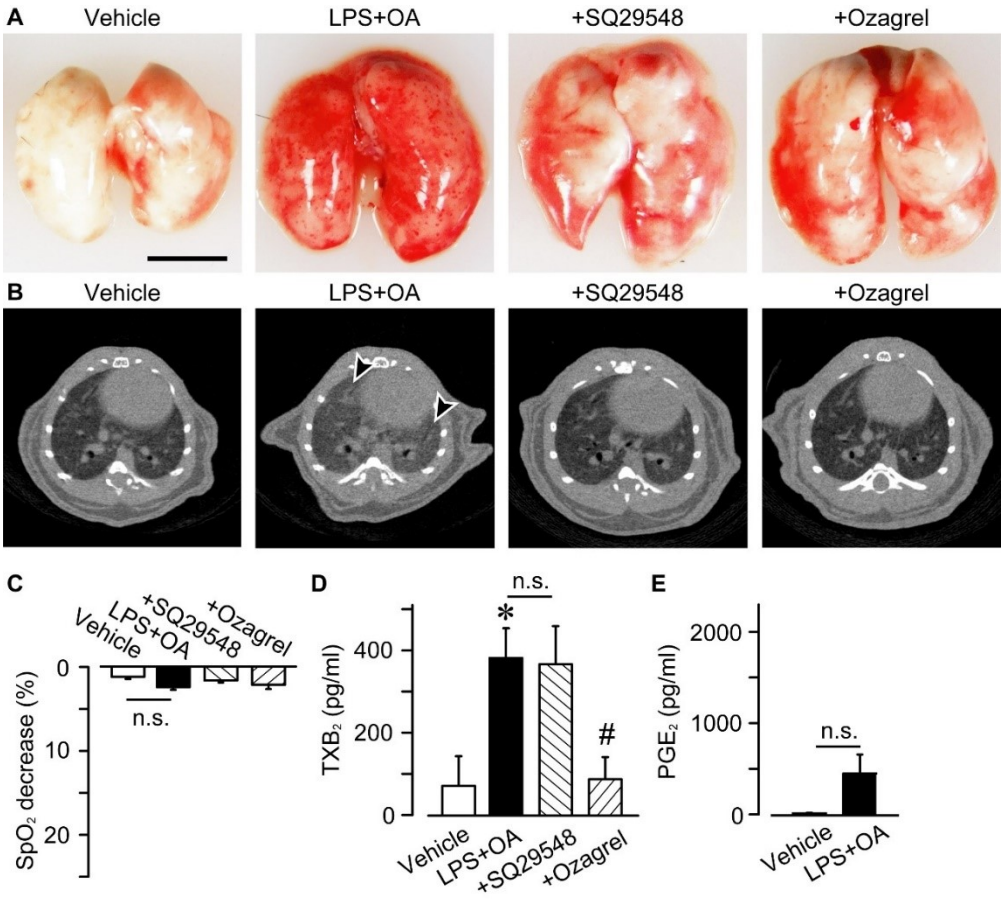

Figure 6. TXS-TXA$_2$-TP signaling aggravated LPS+OA-induced ALI

SQ29548 (2 mg/kg, intraperitoneally, 0, 2, and 4 h after LPS administration) or ozagrel (50 mg/kg, intraperitoneally, 15 min after LPS administration) was treated to LPS (1.5 mg/kg, intra-nasally, 6 h)+OA (150 μl/g, intravenously, 30 min after LPS administration)-induced ALI mice model. (A) Representative pictures of perfused and excised lungs (n=5-10). Bar = 5.0 mm. (B) Representative pictures of the cross section of inflamed lung scanned by CT (n=4-7) Arrowheads indicate infiltrative shadow. (C) Summary of SpO_2 (n=4-6). (D-E) The concentration of (D) TXB_2 (n=5 each) and (E) PGE_2 (n=5 each) in BALF. Data are represented as mean ± SEM. *p<0.05 compared with vehicle-administrated group. #p<0.05 compared with HCl-administrated group. n.s., not significant.

2-6-2 The role of TXS-TXA_2-TP signaling in LPS+OA-induced edema formation and neutrophil accumulation

In the morphological study, LPS+OA-administration caused disruption of alveolar wall accompanied with protein extravasation (black arrowheads) and neutrophil accumulation (white arrowheads, Fig. 7A), which were also observed in HCl-induced ALI model. In addition, the administration of LPS+OA increased both water content and MPO activity (Fig. 7B and C). Both the treatment with SQ29548 and ozagrel significantly decreased water content, but not MPO activity.

These results indicate that TXS-TXA_2-TP signaling aggravates LPS+OA-induced ALI via edema formation, but not via neutrophil accumulation.

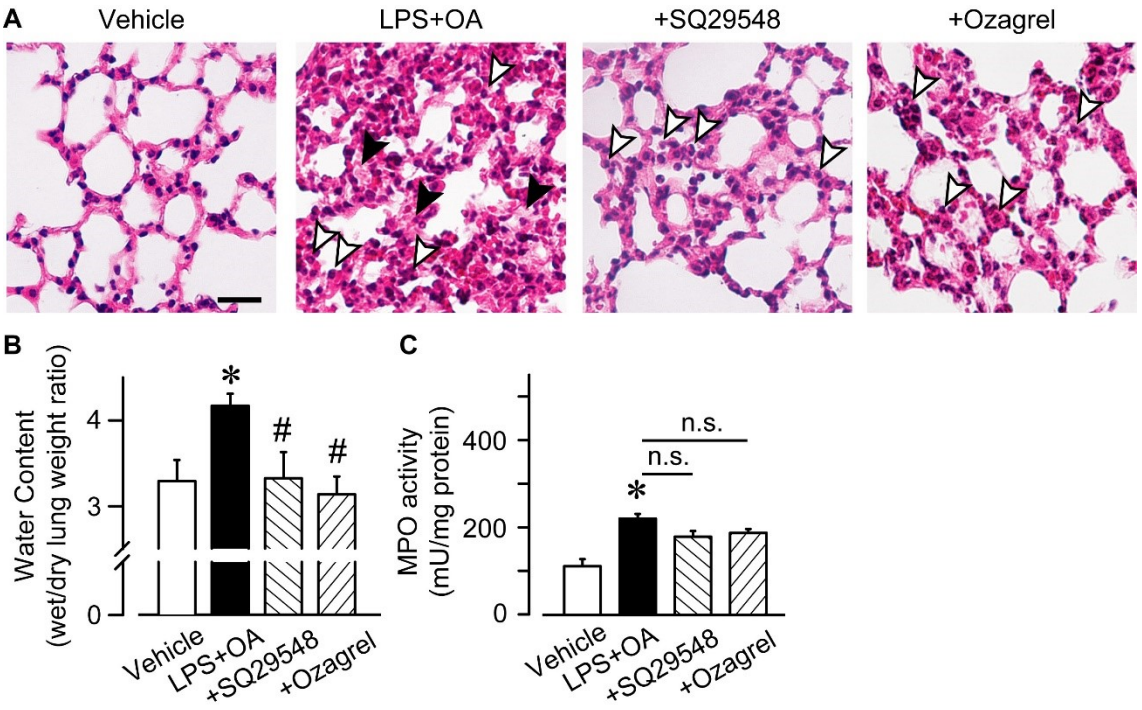

Figure 7. TXS-TXA$_2$-TP signaling promoted edema formation in LPS+OA-induced ALI

SQ29548 (2 mg/kg, intraperitoneally, 0, 2, and 4 h after LPS administration) or ozagrel (50 mg/kg, intraperitoneally, 15 min after LPS administration) was treated to LPS (1.5 mg/kg, intra-nasally, 6 h)+OA (150 μl/g, intravenously, 30 min after LPS administration)-induced ALI mice model. (A) Representative pictures of H&E stained lung section (n=7 each). Black arrowheads indicate protein extravasation and white arrowheads indicate neutrophil accumulation. Bar = 20 μm. (B) Summary of water content (n=5-7). (C) Summary of MPO activity (n=8 each). Data are represented as mean ± SEM. *p<0.05 compared with vehicle-administrated group. #p<0.05 compared with HCl-administrated group. n.s., not significant.

2-7 The role of TXA_2-TP signaling in LPS-induced ALI

2-7-1 The role of TXA_2-TP signaling in LPS-induced ALI

In order to clarify the role of TXA_2-TP signaling in neutrophil accumulation, I utilized LPS-induced ALI model which is known to cause neutrophil accumulation rather than edema formation. The administration of LPS (3.75 mg/kg, intra-nasally) caused inflammation around bronchi (black dotted line, Fig. 8A), but not cause lung dysfunction (Fig. 8B). The treatment of SQ29549 did not affect the area of inflammation.

LPS administration induced the production of BALF TXB_2 and PGE_2 (Fig. 8C and D). However, the level of BALF TXB_2 in LPS-induced ALI model (LPS, 36 ± 24 pg/ml) was lower than that in HCl- and LPS+OA-induced ALI model.

These results suggest that TXA_2-TP signaling does not contribute to LPS-induced ALI progression.

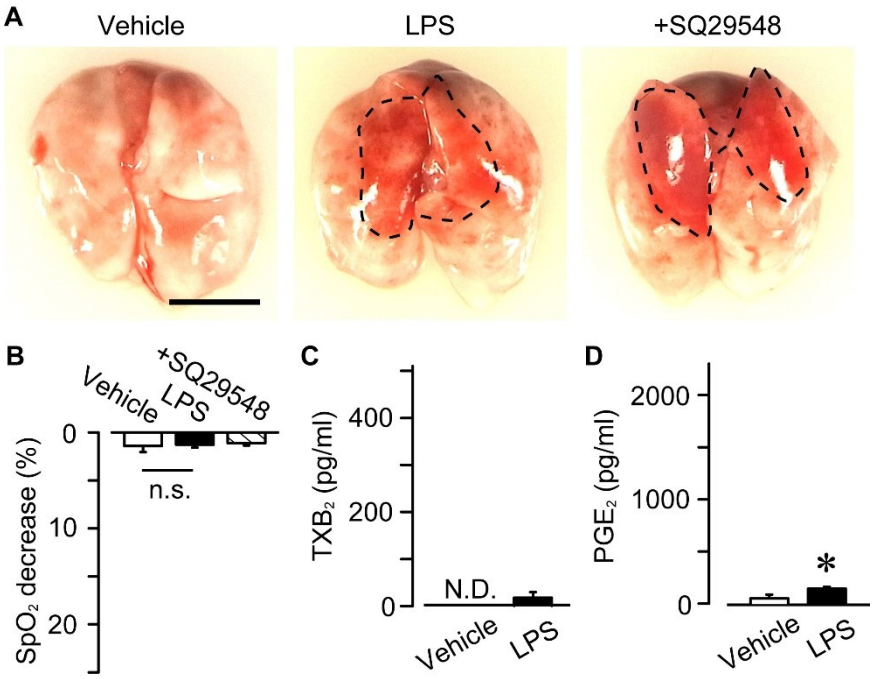

Figure 8. TXA_2-TP signaling did not aggravate LPS-induced ALI

SQ29548 (2 mg/kg, intraperitoneally, 0, 2, and 4 h after LPS administration) was treated to LPS-induced ALI mice model (3.75 mg/kg, intra-nasally, 6 h). (A) Representative pictures of perfused and excised lungs (n=5-10). Black dotted line indicates the area of inflammation. Bar = 5.0 mm. (B) Summary of SpO_2 (n=4-6). (C-D) The concentration of (C) TXB_2 (n=5 each) and (D) PGE_2 (n=5 each) in BALF. Data are represented as mean ± SEM. *$p<0.05$ compared with vehicle-administrated group. n.s., not significant.

2-7-2 The role of TXA_2-TP signaling in LPS-induced neutrophil accumulation

In the morphological analysis, LPS-administrated lung showed severe neutrophil accumulation (white arrowheads), but not protein extravasation (Fig. 9A). In addition, LPS-administration increased only MPO activity, but not water content (Fig. 9B and C), which were not affected by the treatment with SQ29548.

These results indicate that TXA_2-TP signaling is not important in LPS-induced ALI model.

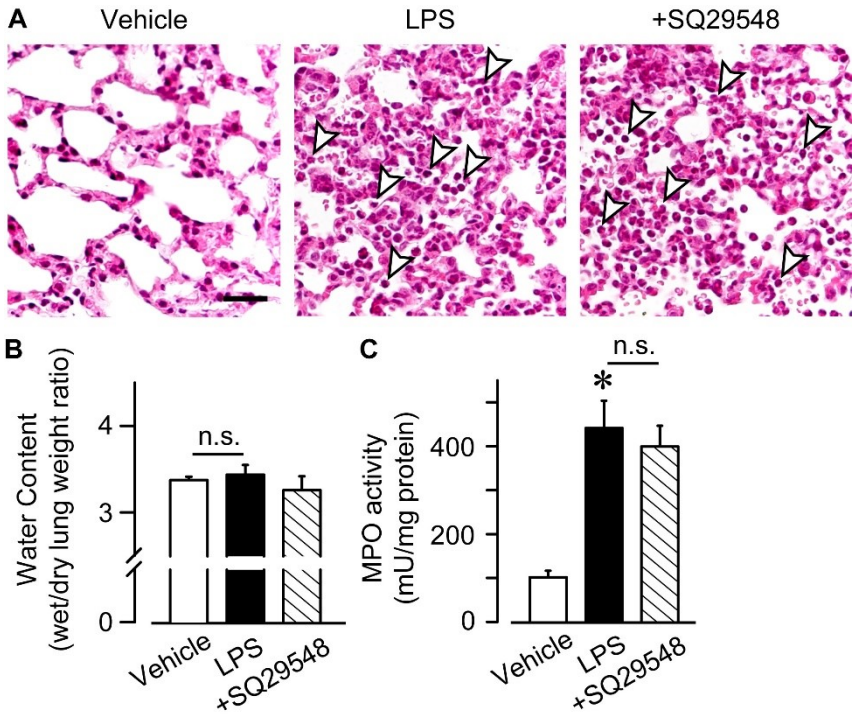

Figure 9. TXA$_2$-TP signaling did not affect in LPS-induced ALI symptoms

SQ29548 (2 mg/kg, intraperitoneally, 0, 2, and 4 h after LPS administration) was treated to LPS-induced ALI mice model (3.75 mg/kg, intra-nasally, 6 h). (A) Representative pictures of H&E stained lung section (n=7 each). White arrowheads indicate neutrophil accumulation. Bar = 20 μm. (B) Summary of water content (n=5-7). (C) Summary of MPO activity (n=8 each). Data are represented as mean ± SEM. *p<0.05 compared with vehicle-administrated group. n.s., not significant.

2-8 The role of TP signaling in vascular hyper-permeability

2-8-1 The role of TP signaling in vascular hyper-permeability

Here I investigated the effect of TP signaling on vascular permeability *in vivo*. I injected Evans blue (50 mg/kg, intravenously, 30 min) after the administration of TP agonist (U46619, 20 or 200 μg) to the right auricle of mice. U46619 administration caused dye extravasation indicating increase of vascular permeability in a dose-dependent manner (Fig. 10A and B). This result shows that TP signaling induce vascular hyper-permeability *in vivo*.

I next evaluated the effect of TP signaling on vascular hyper-permeability and vasocontraction in mice ear. There are various types of vessels in mice ear; proximal vessels, distal vessels, and capillaries (Fig. 10C). In proximal vessels or distal vessels, endothelial cells are covered with vascular mural cells; vascular smooth muscle cells or pericytes. On the other hand, in capillaries, endothelial cells in capillaries are not covered with the mural cells. Intravital microscopy showed that the administration of U46619 (20 μg/ear, 15 min) caused the leakage of FITC dextran (50 mg/kg, intravenously injected) in capillary, but not in proximal vessels or distal vessels (Fig. 10D and data not shown). This result suggests that TP signaling induces vascular hyper-permeability in vascular mural cell-poor vasculatures.

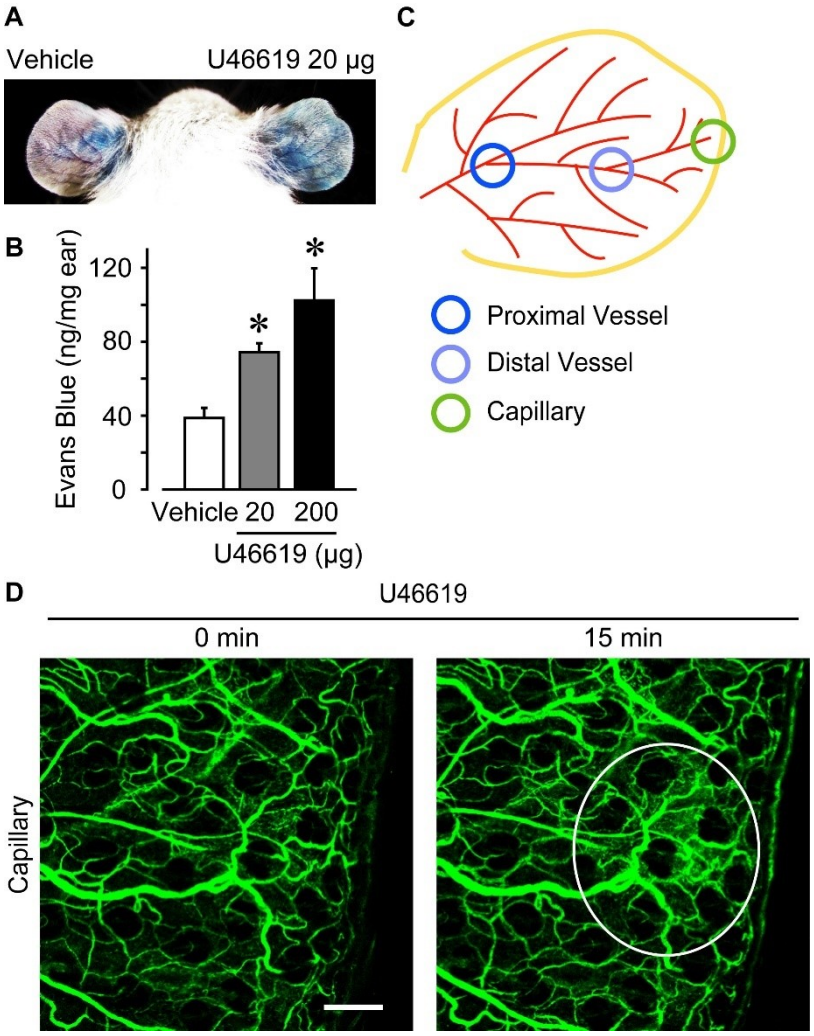

Figure 10. TP signal promoted vascular hyper-permeability

(A-B) Vehicle (methyl acetate, 20 μl) and U46619 (20 or 200 μg) was applied on mice auricles followed by the injection of Evans blue dye (50 mg/kg, intravenously, 30 min). (A) Representative pictures of Miles assay. (B) Summary of dye extravasation (n=4 each). (C) Illustration of vessel of mouse auricle. (D) U46619 (20 or 200 μg) was applied on the auricle of mice flowed with FITC dextran (40 mg/kg, intravenously) for 15 min. Representative pictures of the visualized vessels in the mouse auricle. Data are represented as mean ± SEM. *$p<0.05$ compared with vehicle-administrated group.

2-8-2 The role of TP signaling in blood flow

I further investigated the effect of TP signaling on vasocontraction in mice ear. In the proximal vessels, the administration of U46619 (20 μg) acutely induced vasocontraction of vein but not artery (Fig. 11A, B, and C).

In addition, blood-flow imaging exhibited that the administration of U46619 (20 μg/ear, 20 min) significantly decreased the blood flow in proximal vessel, but not capillary (Fig. 11D and E).

These results suggest that TP signaling cause the contraction of proximal vein accompanied with the blood flow decrease, which might attenuate vascular hyper-permeability in ear proximal vessel.

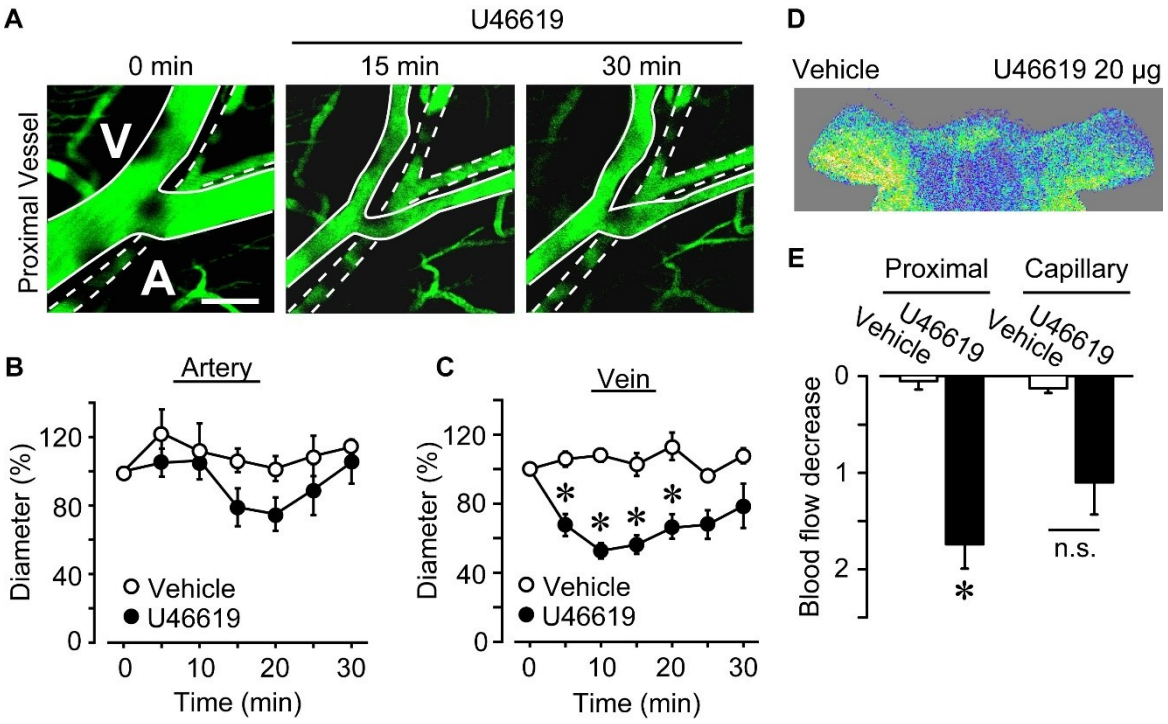

Figure 11. TP signaling decreased the blood flow

(A-C) U46619 (20 μg) was applied on the auricle of mice flowed with FITC (40 mg/kg, intravenously). (A) Representative pictures of the visualized proximal vessels in the mouse auricle. (B and C) Summary of the diameter of (B) artery or (C) vein (n=4-6). (D-E) U46619 (20 μg) was applied on the auricle of mice and the blood flow was measured using laser doppler velocimeter. (D) Representative pictures of mouse. (E) Summary of the blood flow (n=4 each). Data are represented as mean ± SEM. *p<0.05 compared with vehicle-administrated group. n.s., not significant.

2-8-3 The role of TP signaling in endothelial barrier

To regulate vascular permeability, endothelial cells form endothelial barrier via adherence junction composed of VE-cadherin. I next investigated the effect of TP signaling on vascular endothelial barrier *in vivo*.

Whole-mount immunostaining of ear showed that, in control group, ear endothelial cells form endothelial barrier indicated as the localization of VE-cadherin between cell-cell contact areas (Fig. 12A, left panel). The administration of U46619 (20 μg/ear, 15 min) disrupted the localization of VE-cadherin (middle panel, arrowheads). As well as the administration of histamine (400 μg/ear, 15 min, right panel).

En face immunostaining of mouse pulmonary artery showed similar results (Fig. 12B). VE-cadherin was localized between the contact areas in the control group, while the VE-cadherin localization was disrupted in both the treatment with U46619 (1 μM) and histamine (10 μM, arrowsheads).

These results indicate that TP signaling disrupts endothelial barrier *in vivo*.

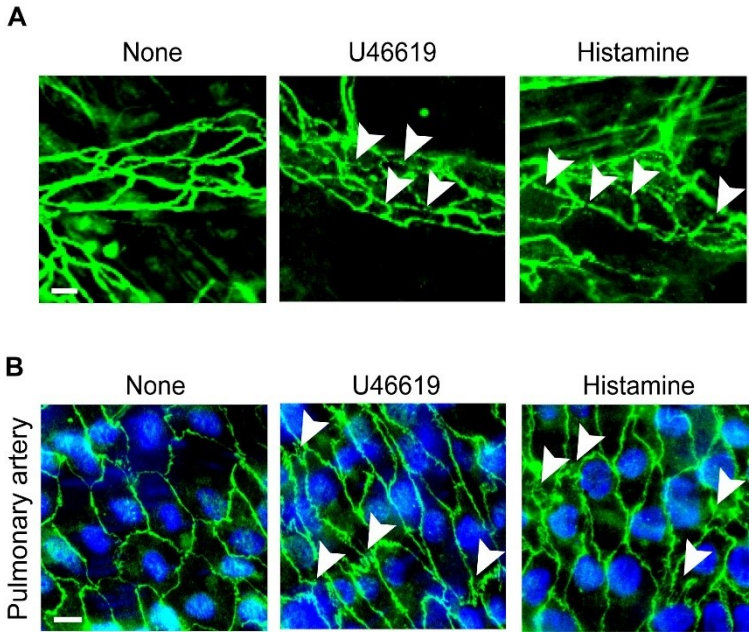

Figure 12. TP signal disrupted endothelial barrier

(A) After the administration of U46619 (20 μg/ear) or histamine (400 μg/ear) for 15 min, ear was excised, fixed, and stained. Representative pictures of whole-mount immunostaining of VE-cadherin (green). Arrowheads indicate endothelial barrier disruption. Bar, 10 μm. (B) Pulmonary artery was excised and stimulated with U46619 (1 μM) or histamine (10 μM) for 15 min. Representative pictures of whole-mount immunostaining of VE-cadherin (green). Nuclei was stained with DAPI (blue). Arrowheads indicate disruption of VE-cadherin localization. Bar, 10 μm.

2-9 The role of TP signaling in endothelial barrier *in vitro*

2-9-1 The role of TP signaling in endothelial barrier *in vitro*

I investigated the mechanism of TP signaling on endothelial barrier disruption *in vitro* using human umbilical vein endothelial cells (HUVECs). The administration of U46619 (0.1-1 μM) decreased the level of trans endothelial resistance (TEndR) and the leakage of FITC-dextran in the dose-dependent manner (Fig. 13A and B). The pretreatment with SQ29548 (1 μM, 30 min before U46619 administration) completely suppressed TEndR decrease by U46619 (Fig. 13C). Furthermore, he 30 min pretreatment with Ca^{2+} channel inhibitor ($LaCl_3$, 5 μM), phospholipase C (PLC) inhibitor (U73122, 3 μM), or Rho kinase inhibitor (Y27632, 10 μM) significantly reduced the U46619-induced TEndR decrease.

These results showed that TP signaling disrupts endothelial barrier via Ca^{2+} channel, PLC, or Rho kinase activity.

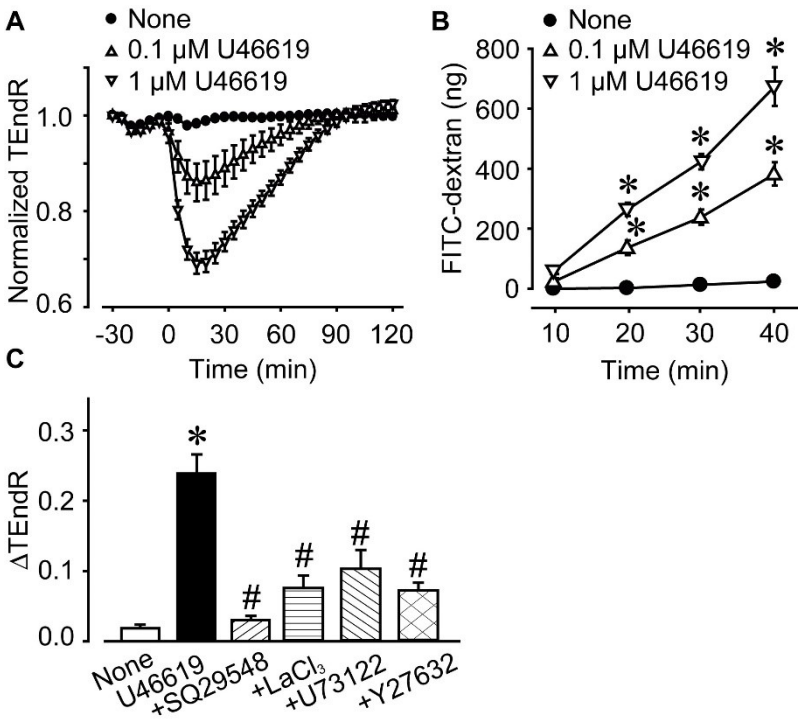

Figure 13. TP signaling disrupted endothelial barrier of HUVECs

U46619 (0.1-1 μM) was administrated onto HUVECs. (A) Summary of TEndR (n=10 each). (B) Summary of FITC-dextran leakage (n=6 each). (C) SQ29548 (1 μM), $LaCl_3$ (5 μM), U73122 (3 μM), or Y27632 (10 μM) was pretreated 30 min before U46619 administration (n=8–14). Summary of the maximum decrease of TEndR. Data are represented as mean ± SEM. *p<0.05 compared with vehicle-administrated group. #p<0.05 compared with U46619-administrated group.

2-9-2 The role of TP signaling in endothelial barrier of HPAECs or HMVECs

I also confirmed that the administration of U46619 (0.01-1 μM) disrupted the barrier of human pulmonary endothelial cells (HPAECs, Fig. 14A and B) and human microvascular endothelial cells (HMVECs, Fig. 14C and D).

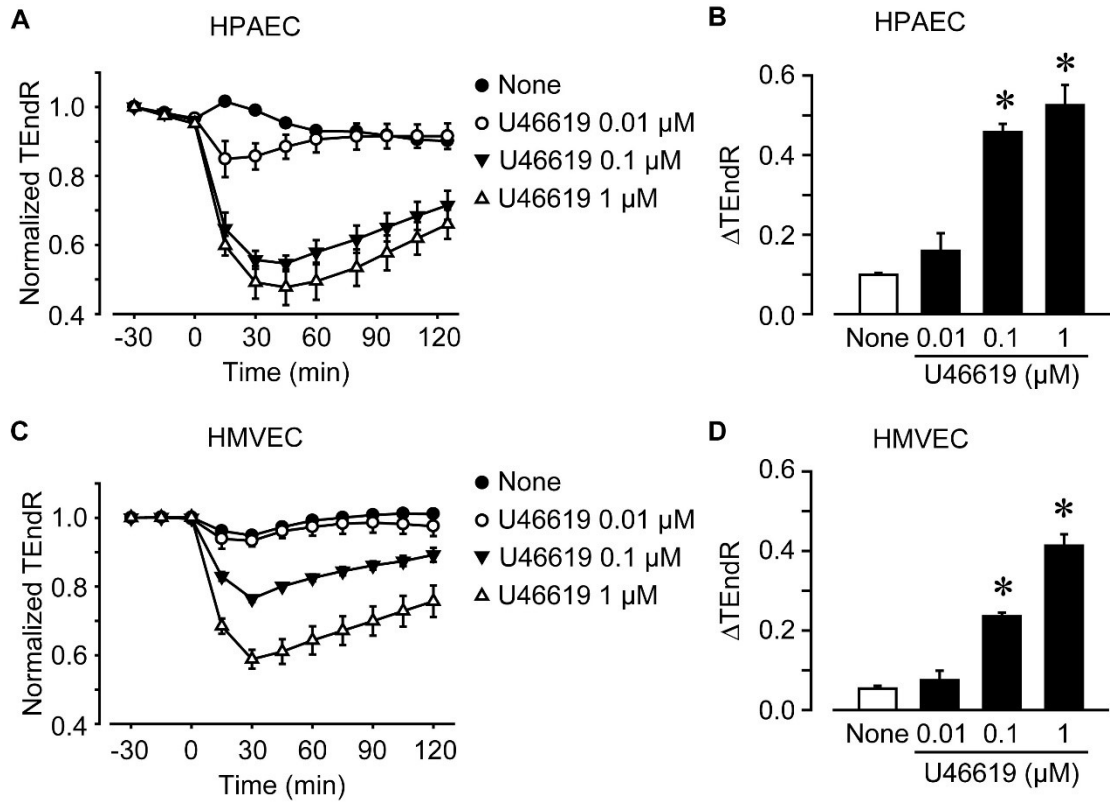

Figure 14. TP signaling disrupted endothelial barrier of HPAECs or HVMECs

U46619 (0.01-1 μM) was administrated onto HPAECs or HMVECs. (A) Change of TEndR of HPAECs. (B) Summary of the maximum decrease of TEndR (n=4 each). (C) Change of TER of HMVECs. (D) Summary of the maximum decrease of TER (n=4-6). Data are represented as mean ± SEM. *p<0.05 compared with vehicle-administrated group.

2-9-3 The role of TP signaling in VE-cadherin localization and cortical actin rim

I performed immunofluorescence assay. In the control group, HUVECs form endothelial barrier composed of VE-cadherin-derived adherence junction and actin-derived cortical actin rim (Fig. 15). The administration of U46619 (1 μM) for 20 min disrupted VE-cadherin localization (arrowheads) and caused stress fiber formation (arrows). The pretreatment with Y27632 (10 μM, 30 min before U46619 administration) inhibited the U46619-induced endothelial barrier disruption.

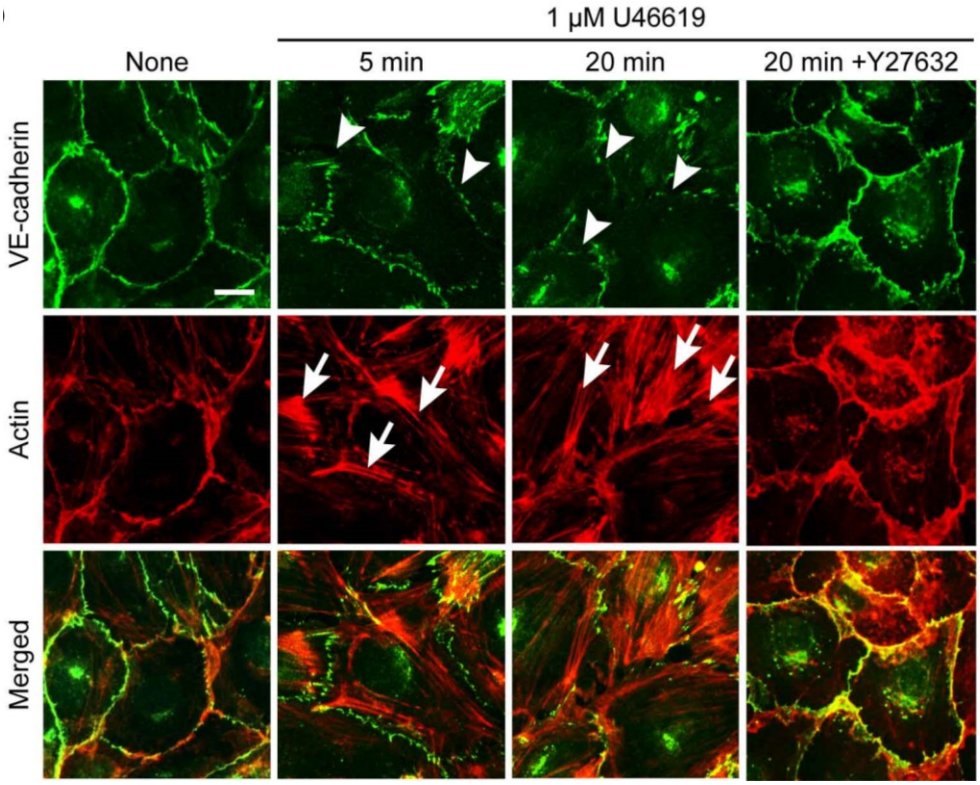

Figure 15. TP signaling disrupted VE-cadherin localization and cortical actin rim

U46619 (1 μM) was administrated onto HUVECs for 20 min. Y27632 (10 μM) was pretreated 30 min before U46619 administration. (A) Representative pictures of immunostaining of VE-cadherin (upper panels, green) and F-actin (middle panels, red, n=4–6). Lower panels show merged pictures. Arrowheads indicate disruption of VE-cadherin localization. Arrows indicate stress fiber formation. Bar, 10 μm.

2-10 Discussion of chapter 2

TXA_2 is one of prostanoids which is known to cause vasocontraction, endothelial barrier formation, and platelet aggregation. Although several studies reported that TXA_2 aggravate ALI progression, the detailed mechanism is unknown. There are urgent needs to clarify the role of TXA_2 signaling in ALI. In this chapter, I here revealed the role of TXS-TXA_2-TP signaling in three types of stimuli-induced ALI progression (Fig. 16).

2-10-1 The contribution of TXS-TXA_2-TP signaling to edema formation

Here I showed that TXS-TXA_2-TP signaling aggravated ALI by promoting edema formation. Using three different ALI models, I found that the level of TXA_2 (measured as BALF TXB_2) is related to that of edema formation (measured as water content, Fig. 17A), but not with that of neutrophil accumulation (measured as MPO activity, Fig. 17B). This relationship supports that TXA_2 is a key regulator of edema formation in ALI.

2-10-2 The role of TXS-TXA_2-TP signaling in neutrophil accumulation

TP antagonism did not affect neutrophil accumulation. Liu *et al.* also showed that TP antagonism by SQ29548 does not reduce neutrophil accumulation significantly.[46] These results support that TXA_2-TP signaling does not contribute to neutrophil accumulation. However, it is known that vascular hyperpermeability promotes neutrophil accumulation. Furthermore, accumulated neutrophils promote vascular hyper-permeability via producing protease and oxygen. It is difficult to divide these symptoms in two.

2-10-3 The type of cells expressing TXS.

In this study, bronchi/alveolar epithelial cells in HCl-administrated lung express TXS, which might be the main source of TXA_2. Previous study showed that HCl administration activates platelet and platelet depletion reduces edema formation accompanied with the significantly, but not completely, decrease of TXA_2 production.[14] In this study, however, I could not observe the increase of platelet number and TXS expression in platelet. The further investigation such as bone marrow transplantation is needed the effect of platelet-derived TXA_2 on ALI.

2-10-4 The difference between three ALI models

In this study, HCl administration caused edema formation and neutrophil accumulation accompanied with lung dysfunction. However, the administration of LPS+OA did not cause lung dysfunction, although the level of edema formation was higher than that in HCl-induced ALI. This contradiction comes from the difference between the pathogenic mechanisms of these two models. It is known that administrated HCl, but not LPS+OA, directly injures type I alveolar epithelial cells which have a crucial role in lung gas exchange. In addition, here I showed that the treatment with TP antagonist did not show the complete inhibition of HCl-induced lung dysfunction although TP signaling is a key regulator of edema formation. Thus, LPS+OA lack the damage of epithelial cells compared with HCl.

The administration of LPS for 6 h did not induce TXA_2 production and edema formation. However, several studies show the LPS-induced edema formation in experimental ALI models.[47-49] In these studies, the term of LPS stimulation is much than 1 Day. Our group previously showed that 3.75 mg/kg LPS administration for 3 days

increased water content in WT mice.[36] Thus, longer stimulation by LPS might induce edema formation and TXA_2 production.

2-10-5 The role of TXS-TXA_2-TP signaling in vascular hyper-permeability

In the present study, TP stimulation causes vasocontraction in proximal vein, while TP stimulation causes vascular hyper-permeability especially in ear capillary accompanied with the endothelial barrier disruption *in vivo*. Lung vasculature is mainly composed of alveolar capillary, which is like ear capillary. Thus, TXA_2-TP signaling might cause vascular hyper-permeability in lung alveolar capillary.

These results suggest that TP signaling has the controversial role in vascular permeability; endothelial barrier disruption and vasocontraction. I here showed that the administration of U46619 onto mice auricle caused vascular hyper-permeability accompanied with the endothelial barrier disruption of ear endothelial cells and the decrease of blood flow via the contraction of proximal vein. I also showed that U46619 administration induced pulmonary edema formation. In HCl-induced ALI model, I showed that TXA_2-TP signaling plays an important role on edema formation. Thus, *in vivo*, TP signaling is a factor of vascular hyper-permeability by disrupting endothelial barrier.

2-10-6 The role of TXS-TXA_2-TP signaling in endothelial barrier disruption

I here showed that the administration of TP agonist disrupt barrier of HUVECs, HPAECs, and HMVECs, which is similar to previous study that TP stimulation disrupts endothelial barrier of bovine aortic endothelial cells and HUVECs.[44,45] TP receptor is known to couple with G_q or $G_{1/13}$ protein.[50] G_q protein signaling induces intracellular

Ca^{2+} influx via Ca^{2+} channel and PLC activation, while G_{12} protein signaling induces Rho kinase activation. Both G_q and G_{12} signaling disrupts endothelial barrier via the stress fiber formation and VE-cadherin internalization.[51] As expected, the pretreatment with inhibitor of Ca^{2+} channel, PLC, and Rho kinase significantly reduced TP stimulation-induced barrier disruption. Thus, in endothelial cell, TP signaling cause barrier disruption via both G_q-derived intracellular Ca^{2+} influx and PLC activation and G_{12}-derived Rho kinase activation.

2-10-7 Summary

In summary, I showed that TXS-TXA_2-TP signaling aggravates ALI via endothelial barrier disruption through Ca^{2+} channel and Rho kinase signaling. These findings may provide new insight to cure the ALI moralism.

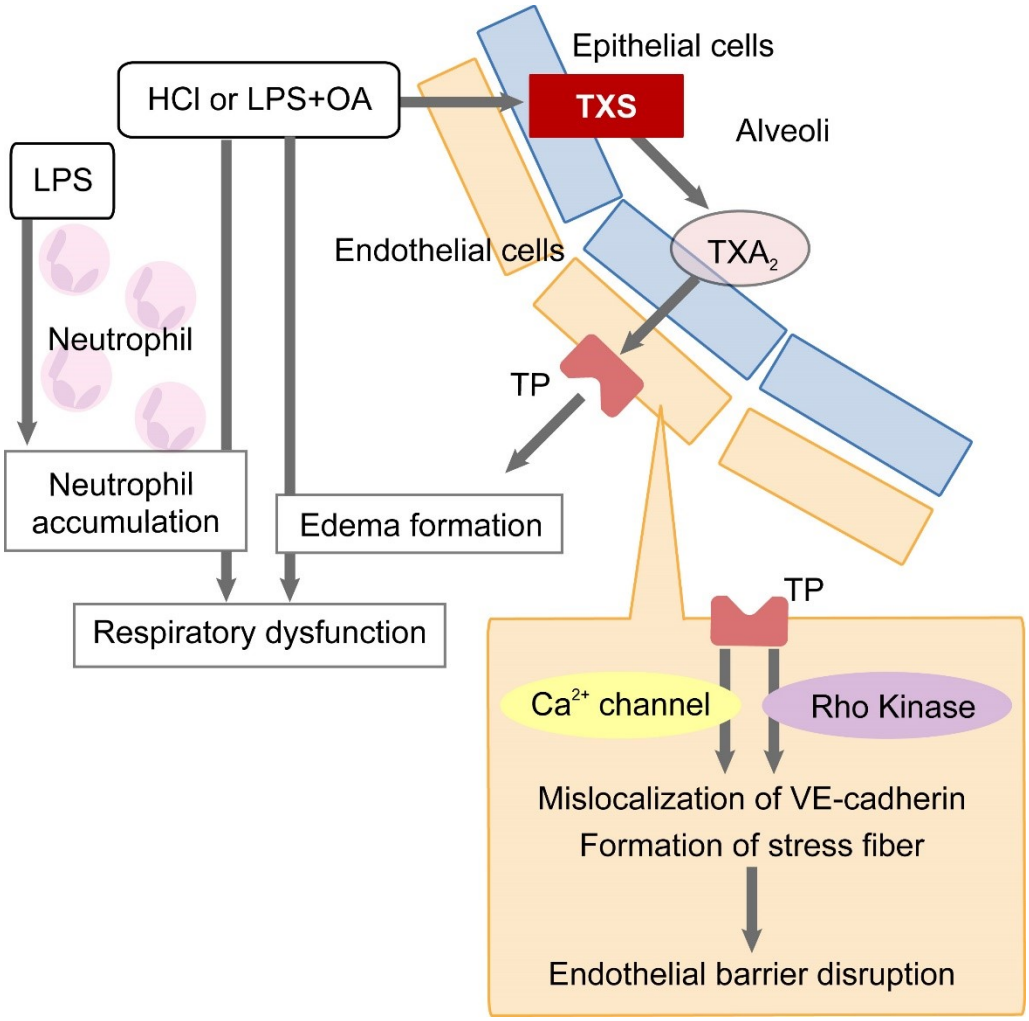

Figure 16. The role of TXS-TXA_2-TP signaling in three ALI models

The administration of HCl and LPS+OA cause lung inflammation accompanied with edema formation and neutrophil accumulation. On the other hand, LPS administration cause only neutrophil accumulation. Inflammatory stimuli cause TXS expression in epithelial cells, resulting in TXA_2 production. TXA_2 binds to TP receptor in endothelial cells, leading endothelial barrier disruption via intracellular Ca^{2+} influx and Rho kinase activation. TXA_2-TP signaling promotes edema formation via endothelial barrier disruption-induced vascular hyper-permeability.

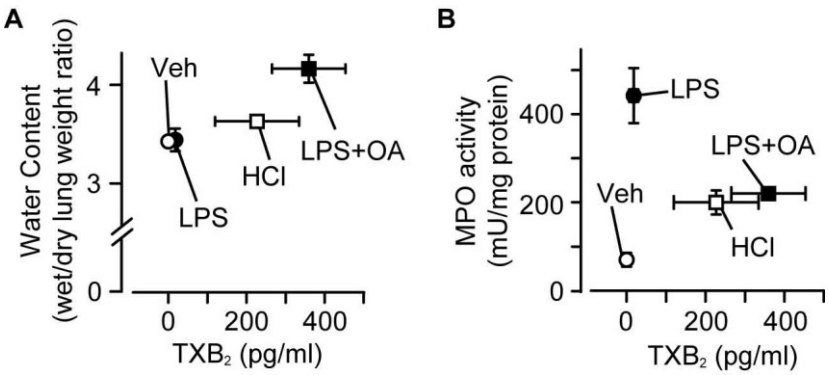

Figure 17. The level of edema formation is related to the level of TXA_2

(A) Scatter plots between the level of BALF TXB_2 and water content (n=4-15). (B) Scatter plots between the level of BALF TXB_2 and MPO activity (n=4-15). Data are represented as mean ± SEM.

【Chapter 3 The role of L-PGDS-derived PGD_2 in ALI】

本章の内容は学術雑誌論文として出版する計画があるため公表できない

5年以内に出版予定

【Chapter 4 Total discussion】

本章の内容は学術雑誌論文として出版する計画があるため公表できない

5年以内に出版予定

【Chapter 5 Summary】

Background and aim

ALI is a lethal respiratory disorder caused by various stimuli such as aspiration of gastric contents, fat embolism, and bacterial mass infection. Although the mortality rate is high, there is no effective pharmacological therapy.

Prostanoids are inflammatory lipid mediators produced by COX. Since these prostanoids are detected in lung tissue of ALI patients, researchers have investigated the therapeutic effect of inhibition on ALI. Although COX inhibition suppress inflammation in the experimental ALI model, COX inhibition did not show the anti-inflammatory effect on ALI in the clinical study. Thus, I need to clarify the role of each prostanoids on ALI progression.

In the present study, I investigated the role of TXA_2 and PGD_2 signaling in ALI progression by using mice ALI models.

Results

I. The role of TXA_2-TP signaling in ALI

TXA_2 is one of prostanoids produced by COX and TXS. It is known that TXA_2 causes platelet aggregation and vasocontraction via its specific receptor, TP receptor. Recently, some studies showed the pro-inflammatory role of TXA_2-TP signaling on ALI progression, the detailed mechanism is still unknown.

I investigated the role of TXA_2-TP signaling in ALI progression by using three different ALI mice models using HCl, LPS+OA, or LPS. The administration of HCl induced hemorrhage accompanied with edema formation and neutrophil accumulation. LPS+OA administration caused severe edema formation and neutrophil accumulation.

The administration of LPS only induced neutrophil accumulation, but not edema formation. In these models, the treatment with TP receptor antagonist suppressed edema formation without affecting neutrophil accumulation. Furthermore, the level of TXA2 production has positive correlation with the level of edema formation.

Immunobiological assay showed that inflamed epithelial cells express TXS. Miles assay showed that the administration of TP receptor agonist caused vascular hyper-permeability by disrupting the endothelial barrier. In vitro assay also showed that TP signaling disrupts endothelial barrier via intracellular Ca^{2+} influx and the activation of Rho kinase.

II. The role of L-PGDS-derived PGD_2 in ALI

PGD_2 is another one of prostanoids produced by COX and its specific synthases; H-PGDS and L-PGDS. H-PGDS is known to be expressed in blood cells and suppress inflammation by producing PGD_2. Our group showed that H-PGDS-derived PGD_2 suppresses ALI progression in LPS-induced ALI mice model. On the other hand, L-PGDS is known to be expressed in central nervous system and the role of L-PGDS-derived PGD_2 in peripheral tissue is unknown.

I investigated the role of L-PGDS-derived PGD_2 in ALI progression by comparing with the role of H-PGDS-derived PGD_2 using HCl-induced ALI mice model. The administration of HCl caused inflammation and respiratory dysfunction accompanied by edema formation and neutrophil accumulation in WT mice. Both L-PGDS- and H-PGDS-deficiency aggravated respiratory dysfunction. In addition, L-PGDS-derived PGD_2 suppressed edema formation, while H-PGDS-derived PGD_2 suppressed neutrophil accumulation. I confirmed the suppression effect of L-PGDS-derived PGD_2 on ALI

progression by using mice which have L-PGDS point-mutation of the active site of PGD_2 production.

Immunobiological assay showed that stimulated epithelial cells and endothelial cells express L-PGDS, while neutrophils strongly express H-PGDS. In addition, the transplantation of WT-derived bone marrow to L-PGDS$^{-/-}$ mice did not rescue aggravated ALI symptoms. Miles assay showed that L-PGDS-derived PGD_2 suppressed HCl-induced vascular hyper-permeability via one of PGD_2 specific receptor, DP receptor. *In vitro* assay showed that DP signaling enhance endothelial barrier, but not epithelial barrier.

Conclusion

In the ALI progression, inflamed epithelial cells might produce TXA_2 via the activity of TXS. Produced TXA_2 binds to TP receptor, resulting in endothelial barrier disruption via the intracellular Ca^{2+} influx and the activation of Rho kinase. The disrupted endothelial barrier cause lung dysfunction by edema formation.

On the other hand, inflamed epithelial cells and endothelial cells produce PGD_2 by the L-PGDS activity. The L-PGDS-derived PGD_2 suppress edema formation by binding to DP receptor in endothelial cells.

This study provides a new insight on ALI progression and leads a novel therapeutic strategy.

【Chapter 6 Reference】

1. The ADTF. Acute Respiratory Distress Syndrome: The Berlin Definition. *JAMA* 2012; **307**: 2526-2533.
2. Ware LB, Matthay MA. The acute respiratory distress syndrome. *The New England journal of medicine* 2000; **342**: 1334-1349.
3. Bellani G, Laffey JG, Pham T*, et al.* Epidemiology, Patterns of Care, and Mortality for Patients With Acute Respiratory Distress Syndrome in Intensive Care Units in 50 CountriesTrends in Acute Respiratory Distress Syndrome in 50 CountriesTrends in Acute Respiratory Distress Syndrome in 50 Countries. *JAMA* 2016; **315**: 788-800.
4. Ashbaugh D, Boyd Bigelow D, Petty T*, et al.* ACUTE RESPIRATORY DISTRESS IN ADULTS. *The Lancet* 1967; **290**: 319-323.
5. Bhandari V, Choo-Wing R, Lee CG*, et al.* Hyperoxia causes angiopoietin 2–mediated acute lung injury and necrotic cell death. *Nature Medicine* 2006; **12**: 1286-1293.
6. Matthay MA, Zemans RL, Zimmerman GA*, et al.* Acute respiratory distress syndrome. *Nature Reviews Disease Primers* 2019; **5**: 18.
7. Hough CL. Steroids for acute respiratory distress syndrome? *Clin Chest Med* 2014; **35**: 781-795.
8. Smith FG, Perkins GD, Gates S*, et al.* Effect of intravenous β-2 agonist treatment on clinical outcomes in acute respiratory distress syndrome (BALTI-2): a multicentre, randomised controlled trial. *The Lancet* 2012; **379**: 229-235.
9. Cornet AD, Hofstra JJ, Swart EL*, et al.* Sildenafil attenuates pulmonary arterial pressure but does not improve oxygenation during ARDS. *Intensive Care*

Medicine 2010; **36**: 758-764.

10. Zeiher BG, Artigas A, Vincent J-L*, et al.* Neutrophil elastase inhibition in acute lung injury: results of the STRIVE study. *Critical Care Medicine* 2004; **32**: 1695-1702.
11. Network TARDS. Ventilation with Lower Tidal Volumes as Compared with Traditional Tidal Volumes for Acute Lung Injury and the Acute Respiratory Distress Syndrome. *New England Journal of Medicine* 2000; **342**: 1301-1308.
12. Guérin C, Reignier J, Richard J-C*, et al.* Prone Positioning in Severe Acute Respiratory Distress Syndrome. *New England Journal of Medicine* 2013; **368**: 2159-2168.
13. Fukunaga K, Kohli P, Bonnans C*, et al.* Cyclooxygenase 2 Plays a Pivotal Role in the Resolution of Acute Lung Injury. *The Journal of Immunology* 2005; **174**: 5033-5039.
14. Zarbock A, Singbartl K, Ley K. Complete reversal of acid-induced acute lung injury by blocking of platelet-neutrophil aggregation. *J Clin Invest* 2006; **116**: 3211-3219.
15. Schuster DP. ARDS: clinical lessons from the oleic acid model of acute lung injury. *American Journal of Respiratory and Critical Care Medicine* 1994; **149**: 245-260.
16. Ishitsuka Y, Moriuchi H, Isohama Y*, et al.* A Selective Thromboxane A2 (TXA2) Synthase Inhibitor, Ozagrel, Attenuates Lung Injury and Decreases Monocyte Chemoattractant Protein-1 and Interleukin-8 mRNA Expression in Oleic Acid–Induced Lung Injury in Guinea Pigs. *Journal of Pharmacological Sciences* 2009; **111**: 211-215.
17. Gonçalves-de-Albuquerque CF, Silva AR, Burth P*, et al.* Oleic acid induces lung

injury in mice through activation of the ERK pathway. *Mediators Inflamm* 2012; **2012**: 956509-956509.

18. Wiener-Kronish JP, Albertine KH, Matthay MA. Differential responses of the endothelial and epithelial barriers of the lung in sheep to Escherichia coli endotoxin. *The Journal of Clinical Investigation* 1991; **88**: 864-875.

19. Liu F, Li W, Pauluhn J*, et al.* Lipopolysaccharide-induced acute lung injury in rats: comparative assessment of intratracheal instillation and aerosol inhalation. *Toxicology* 2013; **304**: 158-166.

20. Kabir K, Gelinas J-P, Chen M*, et al.* Characterization of a murine model of endotoxin-induced acute lung injury. *Shock* 2002; **17**: 300-303.

21. Voelker MT, Fichtner F, Kasper M*, et al.* Characterization of a double-hit murine model of acute respiratory distress syndrome. *Clinical and Experimental Pharmacology and Physiology* 2014; **41**: 844-853.

22. Hinshaw LB, Solomon LA, Erdös EG*, et al.* Effects of Acetylsalicylic Acid on the Canine Response to Endotoxin. *Journal of Pharmacology and Experimental Therapeutics* 1967; **157**: 665-671.

23. Kawasaki M, Kuwano K, Hagimoto N*, et al.* Protection from Lethal Apoptosis in Lipopolysaccharide-Induced Acute Lung Injury in Mice by a Caspase Inhibitor. *The American Journal of Pathology* 2000; **157**: 597-603.

24. Birukova AA, Zagranichnaya T, Fu P*, et al.* Prostaglandins PGE2 and PGI2 promote endothelial barrier enhancement via PKA- and Epac1/Rap1-dependent Rac activation. *Exp Cell Res* 2007; **313**: 2504-2520.

25. Looney MR, Su X, Van Ziffle JA*, et al.* Neutrophils and their Fcγ receptors are essential in a mouse model of transfusion-related acute lung injury. *The Journal*

of Clinical Investigation 2006; **116**: 1615-1623.

26. Cuzzocrea S, Mazzon E, Sautebin L*, et al.* Protective effects of Celecoxib on lung injury and red blood cells modification induced by carrageenan in the rat. *Biochemical Pharmacology* 2002; **63**: 785-795.

27. Göggel R, Hoffman S, Nüsing R*, et al.* Platelet-Activating Factor–induced Pulmonary Edema Is Partly Mediated by Prostaglandin E2, E-Prostanoid 3-Receptors, and Potassium Channels. *American Journal of Respiratory and Critical Care Medicine* 2002; **166**: 657-662.

28. Matthay MA, Eschenbacher WL, Goetzl EJ. Elevated concentrations of leukotriene D4 in pulmonary edema fluid of patients with the adult respiratory distress syndrome. *Journal of Clinical Immunology* 1984; **4**: 479-483.

29. Deby-Dupont G, Braun M, Lamy M*, et al.* Thromboxane and prostacyclin release in adult respiratory distress syndrome. *Intensive Care Medicine* 1987; **13**: 167-174.

30. Looney MR, Nguyen JX, Hu Y*, et al.* Platelet depletion and aspirin treatment protect mice in a two-event model of transfusion-related acute lung injury. *The Journal of Clinical Investigation* 2009; **119**: 3450-3461.

31. Ortiz-Muñoz G, Mallavia B, Bins A*, et al.* Aspirin-triggered 15-epi-lipoxin A4 regulates neutrophil-platelet aggregation and attenuates acute lung injury in mice. *Blood* 2014; **124**: 2625-2634.

32. Bernard GR, Wheeler AP, Russell JA*, et al.* The Effects of Ibuprofen on the Physiology and Survival of Patients with Sepsis. *New England Journal of Medicine* 1997; **336**: 912-918.

33. Kor DJ, Carter RE, Park PK*, et al.* Effect of Aspirin on Development of ARDS in

At-Risk Patients Presenting to the Emergency Department: The LIPS-A Randomized Clinical Trial. *JAMA* 2016; **315**: 2406-2414.

34. Konya V, Maric J, Jandl K*, et al.* Activation of EP4 receptors prevents endotoxin-induced neutrophil infiltration into the airways and enhances microvascular barrier function. *Br J Pharmacol* 2015; **172**: 4454-4468.

35. Birrell MA, Maher SA, Dekkak B*, et al.* Anti-inflammatory effects of PGE2 in the lung: role of the EP4 receptor subtype. *Thorax* 2015; **70**: 740.

36. Murata T, Aritake K, Tsubosaka Y*, et al.* Anti-inflammatory role of PGD2 in acute lung inflammation and therapeutic application of its signal enhancement. *Proc Natl Acad Sci U S A* 2013; **110**: 5205-5210.

37. Cheng Y, Austin SC, Rocca B*, et al.* Role of Prostacyclin in the Cardiovascular Response to Thromboxane A2. *Science* 2002; **296**: 539.

38. Xu S, Jiang B, Maitland KA*, et al.* The Thromboxane Receptor Antagonist S18886 Attenuates Renal Oxidant Stress and Proteinuria in Diabetic Apolipoprotein E-Deficient Mice. *Diabetes* 2006; **55**: 110.

39. Yu M, Tomasa G. A double-blind, prospective, randomized trial of ketoconazole, a thromboxane synthetase inhibitor, in the prophylaxis of the adult respiratory distress syndrome. *Critical Care Medicine* 1993; **21**.

40. Baxter GS, Clayton JK, Coleman RA*, et al.* Characterization of the prostanoid receptors mediating constriction and relaxation of human isolated uterine artery. *British Journal of Pharmacology* 1995; **116**: 1692-1696.

41. McNeish AJ, Jimenez-Altayo F, Cottrell GS*, et al.* Statins and Selective Inhibition of Rho Kinase Protect Small Conductance Calcium-Activated Potassium Channel Function (KCa2.3) in Cerebral Arteries. *PLOS ONE* 2012; **7**: e46735.

42. Spada CS, Nieves AL, Woodward DF. Vascular Activities of Prostaglandins and Selective Prostanoid Receptor Agonists in Human Retinal Microvessels. *Experimental Eye Research* 2002; **75**: 155-163.

43. Daray FM, Minvielle AI, Puppo S*, et al.* Pharmacological characterization of prostanoid receptors mediating vasoconstriction in human umbilical vein. *British Journal of Pharmacology* 2003; **139**: 1409-1416.

44. Klausner JM, Abu-Abid S, Alexander JS*, et al.* Thromboxane modulates endothelial permeability. *Mediators Inflamm* 1994; **3**: 149-153.

45. Kim S-R, Bae S-K, Park H-J*, et al.* Thromboxane A2 increases endothelial permeability through upregulation of interleukin-8. *Biochemical and Biophysical Research Communications* 2010; **397**: 413-419.

46. Liu T, Garofalo D, Feng C*, et al.* Platelet-Driven Leukotriene C4–Mediated Airway Inflammation in Mice Is Aspirin-Sensitive and Depends on T Prostanoid Receptors. *The Journal of Immunology* 2015; **194**: 5061.

47. Xu J, Woods CR, Mora AL*, et al.* Prevention of endotoxin-induced systemic response by bone marrow-derived mesenchymal stem cells in mice. *American Journal of Physiology-Lung Cellular and Molecular Physiology* 2007; **293**: L131-L141.

48. Wadgaonkar R, Patel V, Grinkina N*, et al.* Differential regulation of sphingosine kinases 1 and 2 in lung injury. *American Journal of Physiology-Lung Cellular and Molecular Physiology* 2009; **296**: L603-L613.

49. Zou Y, Dong C, Yuan M*, et al.* Instilled air promotes lipopolysaccharide-induced acute lung injury. *Exp Ther Med* 2014; **7**: 816-820.

50. Huang J. Cell signalling through thromboxane A2 receptors. *Cellular Signalling*

2004; **16**: 521-533.

51. Amerongen GPvN, Delft Sv, Vermeer MA*, et al.* Activation of RhoA by Thrombin in Endothelial Hyperpermeability: Role of Rho Kinase and Protein Tyrosine Kinases. *Circulation Research* 2000; **87**: 335-340.

Acknowledgements

稿を終えるにあたり、まず、実験して頂き、一部資料とデータを提供して頂いた小林幸司特任研究員（Fig. 6A, 6C, 7A-C, 13, and 15）と永田奈々恵特任研究員（Fig. 23-26 Left panels）、遠矢直樹氏（Fig. 18A-B, 20, 21A, 22A, 30, and 31）、山崎愛理沙氏（Fig. 5C）に心より感謝を申し上げます。

また、懇切な御指導及び助言を賜りました東京大学大学院　放射線動物科学研究室　村田幸久准教授と中村達朗特任助教両名に心より感謝を申し上げます。最後に、公私にわたり様々な面で協力を頂き、私の研究生活を支えてくださった研究室の室員やOB・OG、友人そして家族に深く感謝致します。そして、本研究を遂行するにあたり、犠牲となった動物たちに心から感謝するとともに、その霊が慰められるように心からお祈り申し上げます。